An-Najah National University

Faculty of Graduate Studies

DEVELOPMENT OF AN OPTIMIZED SCAFFOLD FOR TISSUE ENGINEERING BASED ON THE NON-COVALENT FUNCTIONALIZATION OF CARBON NANOMATERIALS

By

Salsabeel Mamon Odeh

Supervisors

Dr. Mohyeddin Assali

Dr. Naim Kittana

This Thesis is Submitted in Partial Fulfillment of the Requirements for the Degree of Master of Pharmaceutical Sciences, Faculty of Graduate Studies, An-Najah National University, Nablus - Palestine.

2022

DEVELOPMENT OF AN OPTIMIZED SCAFFOLD FOR TISSUE ENGINEERING BASED ON THE NON-COVALENT FUNCTIONALIZATION OF CARBON NANOMATERIALS

By

Salsabeel Mamon Odeh

This Thesis was Defended Successfully on 29/12/2022 and approved by

Dr. Mohyeddin Assali	_____
Supervisor	Signature
Dr. Naim Kittana	_____
Co-Supervisor	Signature
Dr. Hani Naseef	_____
External Examiner	Signature
Dr. Ramzi Shawahna	_____
Internal Examiner	Signature

Dedication

This is dedicated to:

The greatest dad and mum in the whole world for their unconditional love, prayers, endless support, and for raising me to believe that anything was possible

My beloved brothers and sister for being the pillows and cheerleading squad I have needed. I love you to the moon and back

To a very special, my lovely husband Rashid for his continued and unfailing love, supporting all my dreams, and making everything possible. You were always around at times I thought that it is impossible to continue, you helped me to keep things in perspective. I greatly value his contribution and deeply appreciate his belief in me. You make me the happiest wife; I love you endlessly

I consider myself the luckiest in the world to have such a lovely and caring family, standing beside me with their love and unconditional support.

All the people in my life who touch my soul somehow.

Acknowledgment

I want to start by thanking Allah for giving me the strength, willpower, and guidance I needed to complete this research despite all difficulties.

I am greatly indebted to my research guide, Dr. Mohyeddin Assali, who accepted me as his master student and offered me his mentorship. My deepest thanks to Dr. Naim Kittana for his good advice and scientific support. This work would not have been possible without their guidance and involvement.

I would like to thank the rest of the examination committee, for reading my thesis, their insightful comments and suggestions and invaluable criticisms

Thanks to Dr. Muna Hajj Yahya, Department of Physics, Faculty of Science, at An-Najah National University for her collaboration in conductivity measurements.

I'm thankful to the staff of the laboratories of the College of Pharmacy, Science and Medicine for supplying help and assistance. Especially, the supervisor of the laboratories of the College of Pharmacy Mr. Mohammad Arar and the lab workers Tahreer Shtayeh, Linda arar and thankful to the supervisor of laboratories of the College of Medicine Mr. Ahmed Musa and the lab worker mohammad nabeel and abed zarour.

Declaration

I, the undersigned, declare that I submitted the thesis entitled:

DEVELOPMENT OF AN OPTIMIZED SCAFFOLD FOR TISSUE ENGINEERING BASED ON THE NON-COVALENT FUNCTIONALIZATION OF CARBON NANOMATERIALS

I declare that the work provided in this thesis, unless otherwise referenced, is the researcher's own work, and has not been submitted elsewhere for any other degree or qualification.

Student's Name: _____

Signature: _____

Date: _____

List of Contents

List of Tables

List of Figures

List of Schemes

List of Appendices

DEVELOPMENT OF AN OPTIMIZED SCAFFOLD FOR TISSUE ENGINEERING BASED ON THE NON-COVALENT FUNCTIONALIZATION OF CARBON NANOMATERIALS

By

Salsabeel Mamoon Odeh

Supervisors

Dr. Mohyeddin Assali

Dr. Naim Kittana

ABSTRACT

One of the main approaches for tissue engineering for therapeutic purposes involves the utilization of primary cells that are cultured on a biocompatible scaffold with appropriate characteristics. Such tissues aim to maintain and/or restore normal tissue functions. Over the past few years, significant attention has been given to carbon nanomaterials, like carbon nanotubes (CNTs), and their potential applications in generating tissue scaffolds as they tune some of the tissue's physical characteristics such as flexibility, elasticity, and porosity.

A major obstacle to the employment of CNTs in biological applications was the poor limited water dispersibility and cytotoxicity, however, it was found that the functionalization of CNTs adequately with polar functional groups can solve this problem and improve their biocompatibility. Similar benefits could be achieved by coating the CNTs with chitosan, which is biodegradable, biocompatible, and can form porous structures that are appropriate for cell growth.

Therefore, in our project, we aimed to investigate the characteristics of an engineered connective tissue (ECTs) that is composed of primary dermal fibroblasts and collagen hydrogel that is enriched by varying concentrations of noncovalently functionalization multiwall CNTs (MWCNTs) with pyrene moiety and coated with chitosan. The tested concentrations were 0.025%, 0.05%, and 0.1%.

Our data demonstrated that the enrichment of the ECTs with the functionalized MWCNTs significantly increased the electrical conductivity of the tissues in a kind and concentration-dependent manner. Furthermore, the conductivity enhancement was greater with MWCNTs- COOH compared to MWCNTs-NH2, the concentration of 0.025% of MWCNT-COOH was enough to sufficiently enhance the electrical conductivity of the tissue compared to the control tissue. however, this concentration was still associated with some cytotoxicity where it reduces the cell viability by around (20-30) % relative to the control, while there was no significant reduction in viability when adding chitosan to 0.025%MWCNT-COOH, which indicates that chitosan might have a cytoprotective effect against CNT-induced toxicity, in addition to electrical conductivity enhancement.

Keywords: carbon nanomaterials, tissue engineering, chitosan, MWCNT, primary fibroblast.

Chapter one

Introduction

1.1 Regenerative medicine

Regenerative medicine is a recent multidisciplinary science that aims to improve, maintain, or repair the function of tissues and organs. combining living cells, which provide biological functions, with substances that serve as scaffolds for cell proliferation, can be used to regenerate tissues (1).

Regenerative medicine has raised expectations for a variety of current human disorders around the world. Parkinson, Alzheimer's , spine injuries, osteoporosis, and cancer may all be treated in the near future with treatments aimed at regenerating damaged or diseased tissues (2). The development of cell biology, biological chemistry, and biomaterial science has resulted in new tissue and organ engineering choices (3).

1.2 Tissue engineering

Transplanted organs or cells are used to treat patients who have damaged or diseased organs. However, because of the aging population, There is a severe lack of donor organs and tissues. A new area of medicine called "regenerative medicine" treats diseased or damaged organs and tissues. In 1987, at a meeting of the National Science Foundation, the term "tissue engineering" was first used.

Tissue engineering is one of the most important components of regenerative medicine, which builds on the principles of materials engineering and cell transplantation to create biological alternatives that can maintain and/or restore normal tissue function. Tissue engineering is divided into two categories: the first, depends on the body's natural ability for regeneration when using acellular matrices to promote the optimal orientation and direction of new tissue growth, which are typically created by making up artificial scaffolds or extracting cellular components from tissues through mechanical and chemical manipulation to create collagen-rich matrices (4, 5). The second category is the use of matrices with cells, *in vitro* production, or *in vivo* regeneration using scaffolds built of synthetic or natural materials and filled with living cells. In both in vitro and in vivo procedures, cells are loaded onto a porous scaffold. On the scaffold surface, the nanometer-scale topographical structure can be produced. To improve cell

functions, the scaffold can be functionalized with various chemicals. Components like medications, peptide sequences like arginine–glycine–aspartic acid (RGD), genes, or proteins can be encapsulated in nanoparticles and then released in a controlled manner to reach a specific target like cells, bacteria, or viruses (sheme1) (2, 6).

Scheme 1

Tissue engineering approach for tissue regeneration (2)

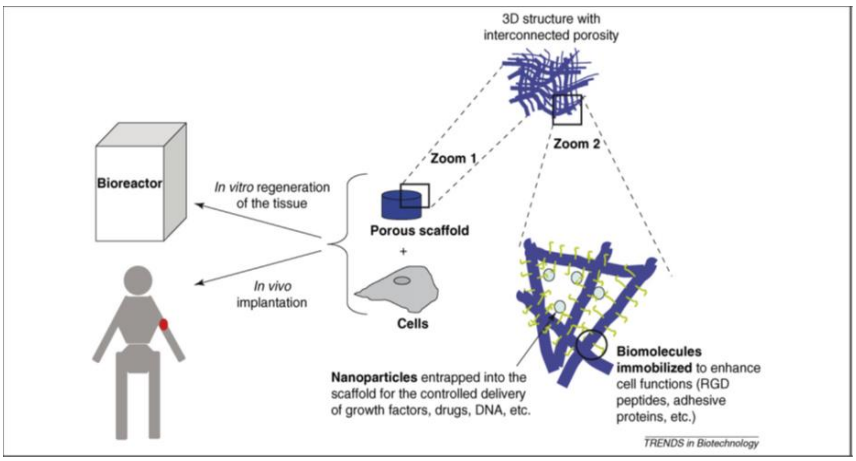

All tissues contain the extracellular matrix (ECM), a non-cellular component., is one of the most essential components in tissue engineering. (7). This environment, which surrounds all cells, is important for normal tissue's function and is also important for tissue regeneration following pathology or damage because it allows cells to grow, move, adhere, proliferate, and differentiate. To enable tissue engineering, the suitable synthetic ECM should identify as closely as possible to the natural ECM . Collagen is a typical biological material used to create a synthetic ECM because it is an abundant protein present in the ECM of body tissues and can provide binding sites to help cells adhere, migrate, proliferate, and differentiate (8, 9).

Epithelial, muscle, nerve and connective tissue are the four main types of body tissues, which are related but not identical cells that are linked and act together to achieve specific objectives. Epithelial tissue is a protective tissue that makes up the body's outer layer and lines many of its cavities. Smooth, skeletal, and cardiac all are types of muscle tissue that can contract and generate distinct voluntary or involuntary movements. Nerve tissue is divided into central and peripheral types and is responsible for transporting chemical and electrical impulses from the central nervous system and brain

to the periphery and back. The final tissue is connective tissue, which is a biological tissue found in practically every organ and creates a larger part of the skin, muscles, blood vessels, joints, tendons, and ligaments (10, 11). Connective tissue connects and supports other tissues as the term indicates, the characteristics of connective tissue unlike the characteristics of other tissues depend on their cellular elements, the connective tissue is vital for cell migration, mechanical support, directing metabolic processes in other tissues, and wound healing. Connective tissues are mainly composed of fibroblasts, collagen fibers, and extracellular matrix (ECM), however, the kind of intracellular matrix changes depending on the type of connective tissue (11). Because of the low inherent healing ability of connective tissue, certain injuries are a typical therapeutic challenge, requiring the development of a scaffold that preserves normal tissue function (12). One of the challenges in developing this scaffold is mimicking the qualities of real tissues, which was overcome by integrating customized nanoparticles into these scaffolds (13, 14).

Carbon nanomaterials are one of the most often used nanoparticles in scaffolds because they share characteristics with a natural extracellular matrix such as flexibility, elasticity, and porosity with similar sizes (15-17). Electrical conductivity is another remarkable attribute of carbon nanomaterials. This characteristic is responsible for improving the electrical connection between cells, resulting in a better connective cardiac tissue engineering (15, 18).

Finally, the functionalized carbon nanomaterials may be coupled with polymeric hydrogels, such as collagen, to create new scaffolds that match the composition and characteristics of the ECM as closely as possible, thus enhancing cell proliferation in injured tissue (19). Therefore functionalized carbon nanotubes can be used as nanomaterials for tissue regeneration (20, 21). Both collagen and functionalized carbon nanomaterials are used to create these scaffolds, which have several advantages. They are bioresorbable, biodegradable, and biocompatible, as well as having the requisite mechanical stiffness and electrical conductivity while preserving a porous three-dimensional nanostructure (20).

Chitosan is also biocompatible, biodegradable, and may be molded into a variety of geometries and has antibacterial activity, chitosan also forms porous structures that are appropriate for cell growth. Because of its biodegradability and biocompatibility, chitosan is a good choice for a number of tissue engineering applications. To improve the mechanical strength of these composites, recently combined chitosan with carbon nanotubes (22). The combination of these characteristics enables the target cells to adhere to the scaffold surface, proliferate and differentiate. These one-of-a-kind scaffolds can help regenerate several tissue types, including skin and myocardium (23).

1.3 Carbon nanomaterials (CNMs)

Carbon nanomaterials are one of the most extensively researched and utilized nanomaterials with diameters between 1 to 100 nm. These include nano-diamond, graphene nanosheets, fullerene (or Buckyball), graphene quantum dots (GQDs), graphene oxide (GO), carbon nanotubes (single-walled and multi-walled), amorphous nanocarbon, and carbon foam are some examples of CNMs (figure1.1). CNM families have special features that can be used in a variety of biological applications (24). CNTs are one of the highly searched carbon nanomaterials in the scientific world due to their unique thermal, mechanical and electrical characteristics (25).

Figure 1.1

types of carbon nanomaterials (24)

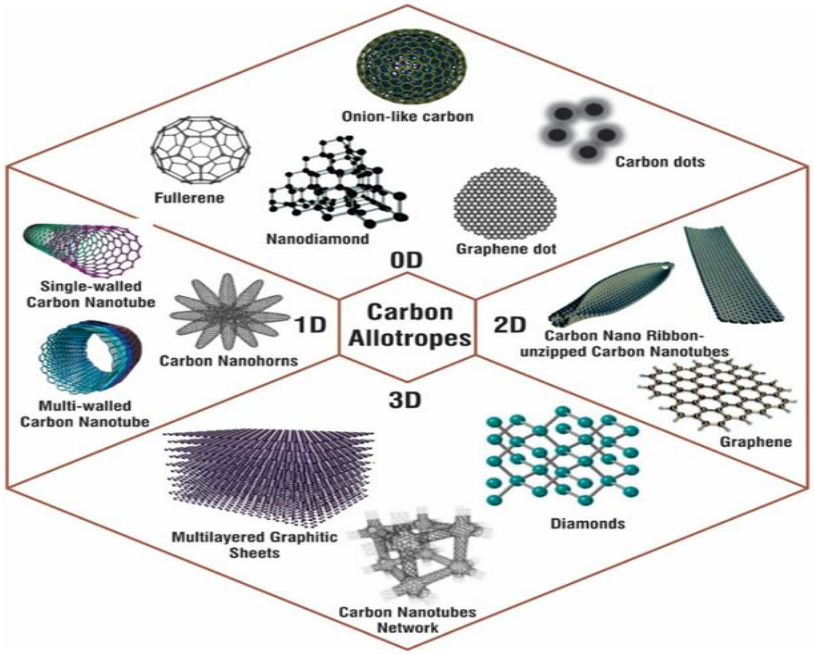

1.3.1 Types of carbon nano allotropes

- **Fullerenes**

The third carbon allotrope, known as buckminsterfullerene (C60), was identified in 1985. Fullerene molecules are hollow spheres or tubes made of carbon atoms. Buckyballs are another name for the bucky forms of spherical fullerenes. It is considered that their three-dimensionality, length, hydrophobicity, and electrical configurations make them an interesting topic in medicinal chemistry (26).

- **Nanodiamonds**

Carbon nanoparticles called nanodiamonds (NDs) have a curved octahedral architecture and are typically 2 to 8 nm in diameter. The surface of nanodiamonds is often covered with a layer of functional groups that reduces dangling bonds and stabilizes the particle. The particles become more stable as a result of the conversion of sp3 hybridization carbon with sp2. The bulk of surface atoms are terminated by groups containing oxygen. While most nanodiamonds are spherical in shape, some of them contain facets (27).

- **Carbon Quantum Dots**

Carbon nanoparticles with a size of fewer than 10 nanometers are known as carbon quantum dots (CQDs). Due to its qualities of being water-dispersible, non-toxic, and fluorescence, CQDs have recently been the topic of research. Graphene, cellulose, and other materials can be used to create CQDs at high temperatures and pressures. CQDs have drawn a lot of interest because of their unique features (28).

- **Graphene**

An allotrope of carbon called graphene is composed of a single sheet of atoms arranged in a two-dimensional hexagonal arrangement. The term, which is a mix of "graphite" and the suffix -ene, relates to the carbon allotrope made up of stacked layers of graphene known as graphite. A hexagonal lattice of sp2-hybridized carbon atoms forms the two-dimensional sheet known as graphene. Due to its mechanical, electrical, and thermal properties, graphene has become extremely popular in both the scientific and technical fields (29).

- **Carbon Nanotubes**

Carbon nanotubes are members of the CNM family. The use of carbon nanoparticles in pharmaceuticals has attracted a lot of attention. This is a result of their highly flexible characteristics plus a few good attributes that they inherently have (24).

1.4 Carbon Nanotubes (CNTs)

In the periodic table, carbon is one of the basic elements. that is necessary for life on Earth to exist. It's also critical for a wide range of technical uses, from pharmaceuticals to synthetic materials (30). Carbon nanotubes (CNTs) are synthetic carbon allotropes (30, 31), also called buckytubes, are nanoscale hollow carbon tubules. They are described as sheets of graphene formed of a hexagonal lattice of condensed benzene rings that have been rolled into a seamless tubule and concentric cylinder with diameters in the range of 5–350 nm and lengths in the micrometer range (32). These cylindrical carbon molecules typically have aspect ratios (length-to-diameter values) greater than 103 (24).

several techniques have been documented for the synthesis of CNTs but the most popular techniques are arc-discharge, laser ablation, and chemical vapor deposition (CVD). The two main types of CNTs are single-walled carbon nanotubes (SWCNTs) and multi-walled carbon nanotubes (MWCNTs) (31, 32). In 1991, Graphitic carbon microtubules with outer diameters of 4 to 30 nm and lengths of up to 1 mm were found. These tubules were made up of two or more concentrically arranged seamless graphene cylinders. These tubes are called MWCNTs (multi-wall carbon nanotubes). While single-wall carbon nanotubes (SWCNTs) are first described in 1993. Which are made of only one seamless cylinder of the graphene sheet (Fig. 1.2). Their lengths are typically in the micrometer range, and their diameters range from 0.4 to 2-3 nm (33).

Figure 1.2

carbon nanotubes structures: A) SWCNTs; B) MWCNTs (34, 35)

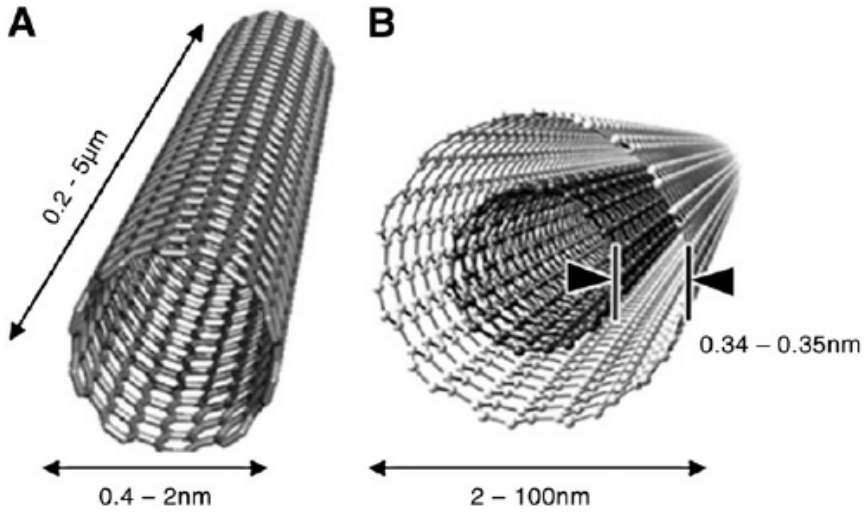

1.4.1 DIFFERENT TECHNIQUES FOR CARBON NANOTUBES SYNTHESIS

To create MWNTs or SWNTs, a variety of procedures are used. Widely used processes for producing CNTs include electric arc discharge, laser vaporization, and chemical vapor deposition. In the sections below, these techniques are described.

1.4.1.1 Electric-Arc Discharge

Often, carbon nanotubes (CNTs) are made by creating an arc between graphite electrodes in an inert environment (argon or helium), a procedure that also results in fullerene-containing carbon soot (36). The carbon arc offers a traditional and practical method for producing the high temperatures (>3000oC) required to evaporate carbon atoms into plasma. The stability of the plasma produced between the electrodes, the current density, the pressure of the inert gas, and the cooling of the electrodes and chamber all affect the yield of the CNTs.

Helium (He) produces the greatest results when compared to the other inert gases, likely because of its high ionization potential. In the arc growth procedure, the well-cooled electrodes and arc chamber serve to enhance the yield of nanotubes. For making MWNTs, the parameters are set up to reduce soot creation during arc evaporation and to produce 75% of the evaporated carbon from pure anodes to deposit onto the graphite cathode surface.

The arc deposit is composed of an internal soft black powder formed of around two-thirds CNTs and one-third graphitic nanoparticles, and an exterior hard gray shell built of pyrolitic graphite. The ideal synthesis conditions were 20-25V, 50-100Amp direct current, and 500 torr of helium pressure. The arc discharge is a quick and easy procedure that produces high-quality CNTs with excellent structural properties. Conventional arc discharge, on the other hand, is a discontinuous and unstable process and cannot produce a significant amount of CNTs. When the CNTs are made on the cathode surface and the electrode spacing varies, neither the current flow nor the electric fields are homogeneous. As a result, carbon nanoparticles and contaminants always coexist with nanotubes and the density of carbon vapor and temperature distribution are not uniform. Many efforts have been made to create a steady and highly effective discharge, and numerous studies have been conducted to understand the nanotube development mechanism.

The arc method typically uses high-purity graphite electrodes, metal powders (only for creating SWNTs), and high-purity He and Ar gases; as a result, the cost of producing SWNTs and MWNTs is expensive. Although the material has a high degree of crystallinity, the length and diameter of the tubes cannot be controlled. Unfortunately, other by-products are also produced, including amorphous carbon, polyhedral graphite particles (in MWNTs), and encapsulated metal particles (in SWNTs) (37).

1.4.1.2 Laser Vaporization

The laser evaporation method is a productive way to create bundles of SWNTs with a limited distribution. With this technique, a graphite target is heated to a high temperature and exposed to an argon atmosphere before vaporizing under laser irradiation. When a pure graphite target was used, MWNTs were discovered. The yield and quality of these products have been proven to be temperature-dependent. At a reaction temperature of 1200oC, the greatest quality is produced. Lower temperatures cause the structural quality to decrease and the CNTs to begin showing numerous defects. When small amounts (a few percent or less) of transition metals (Ni, Co) acting as catalysts are added to the graphite pellet, the results undergo dramatic changes, and SWNTs rather than MWNTs are produced.

The type of metal catalyst employed and furnace temperature are two important variables that have a significant impact on the yield of SWNTs. In the condensing vapor

in a heated flow tube, a high yield with around 50% conversion of transition-metal/graphite composite rods to SWNTs was recorded (operating at 1200oC).

Due to the utilization of high-purity graphite rods, the high laser strengths required (in some circumstances, two laser beams are needed), and the lower daily production of CNTs compared to the arc discharge approach, the laser technique is not an economically viable (37, 38).

1.4.1.3 Chemical Vapor Deposition

One of the most used techniques for depositing thin films is chemical vapor deposition (CVD). The two other popular techniques for making CNTs, electric arc discharge, and laser vaporization, are very different from CVD. Catalytic CVD is a medium temp (700-1473K) and long-time reactions (usually minutes to hours) method, whereas arc discharge and laser vaporization can be categorized as high temperature (>3000K) and short time reaction (s-ms) approaches. Arc discharge and laser vaporization both make CNTs stand-alone materials, which is one of their main technological limitations. CNTs do not develop on a typical or designed substrate.

Although the majority of CVD-grown CNTs were initially "spaghetti-like" and defective, the technique's ability to meet technical needs was understood. Since 1998, significant and quick improvement has been made in CVD, establishing it as a highly regulated process for the creation of CNTs. High quality single-walled carbon nanotubes (SWNTs) and multi-walled carbon nanotubes (MWNTs) can now be produced in bulk as raw material or directly onto substrates.

A significant advantage of CVD is that the CNTs can be employed immediately without additional purification, except for the need to remove the catalyst particle. CNTs are produced using the CVD technique by decomposing an organic gas over a substrate coated in metal catalyst particles. Many CVD techniques are reported, including catalytic pyrolysis of hydrocarbons, thermal CVD, and plasma assisted CVD (37).

- **Thermal Chemical Vapor Deposition (Hydrocarbon Gas Decomposition on Metal Catalysts)**

A quartz tube surrounded by a furnace makes up a thermal CVD reactor, which is easy to build and relatively inexpensive. Si, alumina, silica quartz, and mica are just a few possible substrate materials. By adjusting many parameters, including the hydrocarbon

sources, the type of catalytic metals and their supports, the gas flows, the reaction time, the reaction temperature, etc., the reaction's nature and yield may be regulated. The physical (e.g., length, shape, diameter) and chemical (e.g., flaws, graphitization) features of CNTs can be planned in advance by choosing the appropriate conditions.

Ethylene (C2H4) or acetylene (C2H2) gas is typically employed as the carbon feedstock while Co, Ni, or Fe nanoparticles are used as the catalyst in thermal CVD procedures to generate MWNTs (37).

- **Plasma Enhanced Chemical Vapor Deposition**

The selective positioning and vertical alignment of CNTs can be achieved using the promising upcoming growth technology known as plasma-enhanced chemical vapor deposition (PECVD). Applications that use vertical alignment are crucial. This is especially helpful for field emitters, that are currently being evaluated for use in flat panel displays.

According to conventional wisdom, plasma processing is superior to thermal CVD because the precursor is dissolved by extremely energetic electrons, allowing the substrate temperature to be significantly lower. These techniques make it abundantly clear that PECVD is a high yield and controllable method of creating CNTs with vertical alignment.

- **Catalytic Pyrolysis of Hydrocarbon**

This process is frequently used to produce CNTs in bulk or in large quantities using CVD. The main benefit of utilizing this method is that CNTs can be recovered from the substrate without the need for purification. The easiest way is to directly introduce catalyst nanoparticles into the CVD chamber, for example, in the form of a colloidal/particle suspension or organometallic precursors with a carbon feedstock. Precursors for the catalyst are frequently composed of organometallic compounds, such as iron pentacarbonyl, metallocenes, and iron (II) phthalocyanine. When heated, these precursors often sublime and generate catalyst nanoparticles in the process when the chemical is broken down or reduced by heat or hydrogen. Due to the different temperatures required for nanotube development and organometallic sublimation, a double stage furnace is frequently required.

In general, the structural properties of the nanotubes, like length and diameter, can be only moderately controlled through the sublimation of metallocenes. However, it has been demonstrated that the average diameter of the structures can be altered by altering the reactive concentration of the metallocene to carbon in the gas phase.

The nanotubes are nearly always produced on quartz (SiO2), either as the reactor wall or a particular substrate. This technology has the advantage of producing aligned CNT bundles in a single step at a low cost without the need to prepare substrates before (37).

1.4.1.4 Other Synthesis Techniques for Carbon Nanotubes

Diffusion flame synthesis (39), electrolysis with graphite electrodes submerged in a liquid ionic salts (40, 41), graphite ball milling (42), and heat treating a polymer (37) are further methods for producing CNTs.

1.4.2 Properties of CNTs

One of the most searched carbon nanomaterials by scientists are carbon nanotubes (CNTs), because of their unique features (excellent mechanical characteristics plus thermal and electrical conductivities) (25, 43). CNTs have a nanoscale size and micrometer length, forming a structure like a needle with a large surface area (35), they are lightweight with highly porous materials (44). CNTs have exceptional physical characteristics, MWCNTs have a tensile strength that can reach 63 GPa, about 50 times that of steel . CNTs and their elastic modulus might range from 1.0 to 1.8 terapascals (TPa) (45), and have a mean fracture strength of more than 100 gigapascals (GPa). At room temperature, MWCNTs' thermal conductivity is measured to be more than 3000 WK-1m-1 (46).

Carbon nanotubes possess special electrical characteristics (47), depending on chirality and how the hexagon rings are arranged along the tubular surface, they can either be metallic or semiconductors (48). In SWCNT, the graphene layer can be rolled up in a variety of ways: perpendicular to the face (zigzag tubes), along the face of the hexagon (armchair tubes), and in all intermediate layers (chiral) (figure 1.3) (49).

Figure 1.3

graphene sheet folded in three different patterns: a) chair, b) zigzag, c) chiral (49)

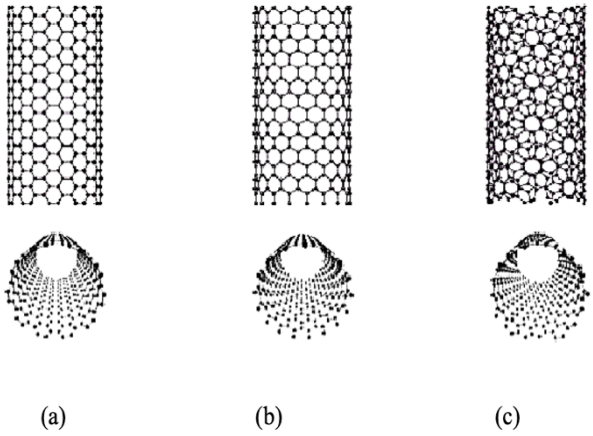

The chirality of nanotubes determines their characteristics including their electronic conductivity. An SWCNT's chirality is determined by the chiral vector Ch, Ch = na1 + ma2, where a1 and a2 are the lattice vectors of graphene while n and m are the graphene's geometrical parameters (scheme 2). for example, When n= m (n, n), SWCNT with an armchair structure will have no band gap and always be metallic. SWCNT adopts a zigzag chirality with either metallic or semiconductive properties when m = 0. If n > m > 0 and n = 3q (q is an integer) metallic chiral-structured SWCNT is also possible (50).

Scheme 2

Figure showing the different graphene rolling directions that can produce single-wall carbon nanotubes with differing chiralities (50)

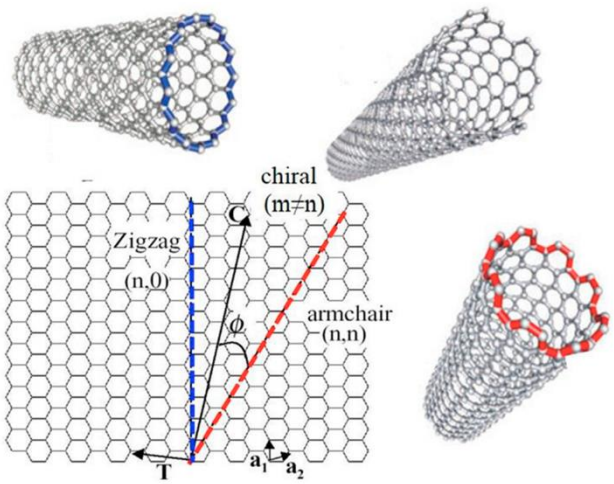

In MWCNTs cylindrical graphene sheets can be described by two structural models: the parchment model (as rolled paper, rolled around itself) and the Russian doll model (single-layer nanotubes coaxially nested into one another) (figure 1.4). When any sheet has metallic chirality, MWCNT is metallic. Because the majority of the current traveling through is restricted to the outermost layer, it has also been shown that the electron transport in MWCNTs is comparable to that of the SWCNTs (50).

Figure 1.4

Multilayer nanotubes' transverse structure is represented schematically: a) Russian doll, b) parchment (49)

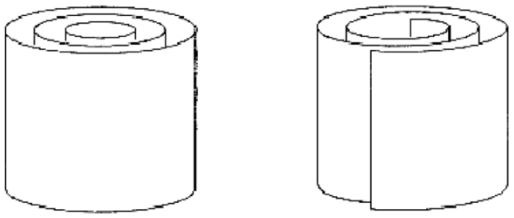

1.4.3 Applications of CNTs

Due to the special characteristics of CNTs, they are extensively studied in a variety of fields, including physics, biology, chemistry, medicine, and engineering. For electrochemical transduction in biosensors, CNTs have been identified as one of the most crucial materials, due to the great surface area that enables signal amplification and chemical stability (51). Additionally, CNTs used for food safety, environmental monitoring, clinical diagnostics, and drug targeting. They are crucial in identifying different pathogenic bacteria and also aid in the treatment of cancer. CNTs even exhibit a variety of antibacterial properties (52). Due to the ability to give the scaffold unique features and steering cell growth, CNTs are an important component in the tissue engineering (53).

- **CNT Use for Diagnostic**

Due to their strong biocompatibility, CNT is being used frequently in biomedical applications, whether for disease diagnosis or treatment.

The development of detection technologies is particularly important because early diagnosis is a necessity for effective therapy. Several teams have examined employing CNTs as the primary component of electrochemical sensors due to their electrical properties, and numerous label-free CNT-based biosensors have been produced as a result. CNT can also act as a contrast agent in several bio-imaging methods. When functionalized and coupled with different biomarkers, they can effectively and accurately identify the presence and location of targeted cells (54).

- **Biosensors Based on CNT**

In the field of biosensors, CNT has been suggested as a sensing component to identify and detect a variety of diseases, mainly diabetes and also bacterial infections. In general, the presence of CNT at the electrode surface accelerates the transport of electrons and increases the sensitivity of the electrochemical detection (55). Recently, resistive sensors, and more specifically differential resistive pulse sensors (RPS) based on MWCNT, demonstrated their remarkable efficacy in passing the single molecule detection threshold (56).

- **Imaging Methods Based on CNT**

There are numerous CNT-based technologies available for use in imaging. In order to penetrate further, photoluminescent imaging, for instance, uses excited SWCNT's fluorescence in the Near InfraRed-I (700–900 nm) and NIR-II (1100–1400 nm) ranges, where tissues and water are practically transparent. This characteristic was employed by Welsher et al. to optically monitor in real time the biodistribution of SCWNTs injected into deep tissues and arteries of mice (57).

- **Tips for scanning probe**

The usage of scanning probe tips is crucial for obtaining images with higher resolutions. When a MWNT-bound scanning probe is employed in place of a standard probe, picture resolution can be improved compared to past results. These probes are now available

commercially by Daiken Chemical Company and Seiko Instruments. Nanotube tips that have been chemically modified can be utilized as sensors to identify particular chemical and/or biological groups. These sensors are crucial for identifying additional or even illicit compounds (58).

- **Targeted Treatments using CNT**

In the medical industry, effective drug administration is a serious challenge. Moreover, low selectivity and short half-lives might result in multiple administrations, which can have side effects and even be toxic. CNT are extensively researched as nanocarriers for drug and gene delivery as well as a cancer treatment because of their expected biocompatibility and acceptable size (54).

- **CNTs as fillers**

One of the most advanced fields in nanotechnology is the use of CNTs as fillers in various materials to create nano-composites. CNTs have been used as a filler by numerous scientists studying nanocomposites. The primary goal of incorporating CNTs into various polymeric and other materials is to enhance their properties. The mechanical, electrical, and thermal properties are raised to their most optimum level as a result.

According to Soichia et al, adding SWNT loading to a SWNTs/polyimide nanocomposite enhanced the material's tensile modulus and yield strength. They demonstrated that the mechanical properties of polyimide were improved with a good dispersion (59).

- **CNT's medical applications**

The science of nanomedicine has developed into the most quickly expanding field of study as a result of the rising profits connected with medical technology related to gene therapy, cancer treatments, and innovative new therapies for life-threatening diseases. Scientists can create new subfields of nanomedicine due to the special characteristics and properties of CNTs. SWNTs and MWNTs have already proved their potential to act as safer and more effective alternatives to earlier drug delivery systems.

They have the ability to cross membranes and deliver vaccinations, nucleic acids, and therapeutic drugs deep inside the cell to their intended substrate sites. They act as the best nontoxic carriers, which in some situations increase the drug's solubility for improved effectiveness and safety. Overall, CNTs have a very promising future in medicine, according to recent studies (58).

1.4.4 Toxicity of CNTs

The use of CNTs in the industry has been considered thoroughly because of their exceptional physical and chemical capabilities, but there are some drawbacks, particularly those linked to their toxicity. To reduce the toxicity of CNTs, specific actions must be taken. Incorporating CNTs into polymeric materials is expected to change their surface characteristics, which may change their toxicity without compromising their unique properties or potential for application in the future. A strategy based on the development of inherently safer nanomaterials, however, appears to have much more potential. Such methods are important for the further improvement and safe application of CNTs, both for professionals and everyday users. It is evident from numerous research on the toxicity of CNTs that surface modifications are essential for decreasing CNT toxicity. And also coating allows for the alteration of the CNTs' external surface environment while preserving their intrinsic structure and essential properties, it may be a useful tool (58).

biological applications have been hampered due to the limited water dispersibility, unfunctionalized CNTs (CNTs free of any polar functional groups) tend to agglomerate together and precipitate in aqueous solutions rather than disperse in water (60, 61). adding the polar functional groups to CNTs can dramatically increase their dispersibility in aqueous conditions while also greatly reducing their toxicity because pristine CNTs may induce a number of toxic reactions (62, 63).

1.4.5 Functionalization of CNTs

CNTs' poor solubility in most organic solvents and aqueous solutions makes them unsuitable for biological applications. As a result, appropriate surface functionalization on CNTs can increase their biocompatibility and ability to disperse in water and thus reduce their toxicity (64). Carbon nanotube cytotoxicity is primarily determined by their

surface functionalization, nanotubes with well-functionalized, serum-stable have the least harmful and toxic effects.

For the functionalization of CNTs, there are two basic protocols: covalent and noncovalent functionalizations (65).

1.4.5.1 Covalent functionalization of CNTs

During chemical reactions, the functional groups are generated, and covalent reactions occur between these groups on the π- conjugated carbon nanomaterial skeleton (65) (scheme 3). The goal of this functionalization approach is to prevent connected biomolecules from being released before they reach the target location, reducing their side effects. The high stability of covalently functionalized carbon nanotubes makes them ideal for drug delivery . covalent functionalization is providing beneficial functional groups on the surface of CNT while maintaining high dispersion stability. Conversely, covalent techniques can result in a huge number of defects on the CNT's sidewall as well as the fragmentation of CNTs with missing inherent properties in the worst situation layers . the covalent method has been observed to disrupt the π-network, resulting in the loss of mechanical and electrical characteristics (66).

There have been numerous reports of successful covalent surface functionalization. The two general strategies of covalent functionalization that result in biomedical applications are nonselective attack of nanotube sidewalls utilising highly reactive species like nitrenes; and the formation of amide bonds at ends of nanotubes using carboxyl group, which is typically generated on CNTs by oxidation in strong acid(67).

Scheme 3

Covalent functionalization of CNTs (43)

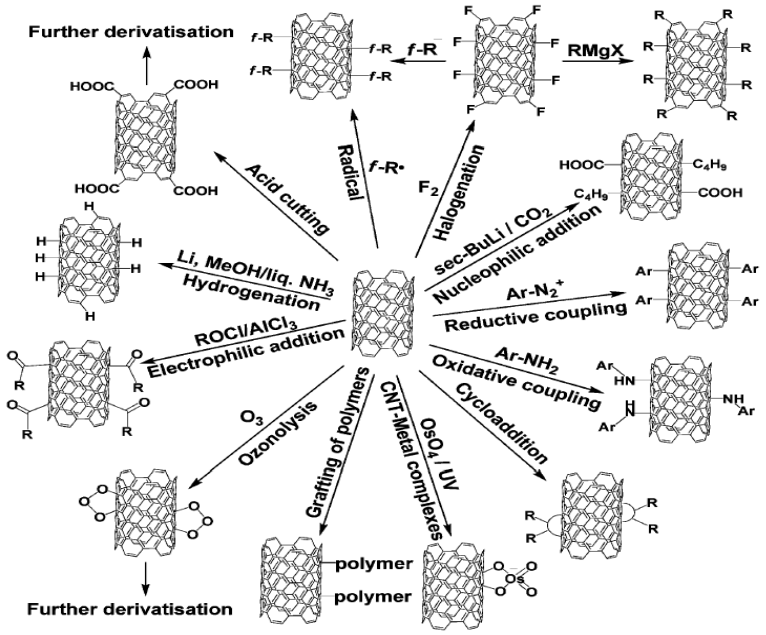

1.4.5.2 Non-covalent functionalization of CNTs

The ability to retain the intrinsic features of CNT while giving additional functionality makes non-covalent functionalization attractive. Non-covalent methods may aid to preserve the conformational structure following immobilization on carbon nanotubes, but covalent methods may alter the carbon nanotubes' sp2 structures, affecting their mechanical and electrical properties. In general, the best method for non-covalent CNT functionalization should include biocompatible functionalization agents which are stable on the CNT surface without detachment in a variety of conditions and have appropriate functional moieties for attaching to various biomolecules (50, 68).

The non-covalent functionalization of CNTs can be done through CH- interaction, van der Waals force (π–π stacking), and s electrostatic interaction between CNTs and biomolecules (65, 69). Dai and coworkers announced the first general and uncomplicated strategy for functionalizing SWCNTs with proteins via π–π stacking (scheme 4) (68). π–π stacking occurs between the sidewall of the SWCNTs and the pyrenyl group of the bifunctional 1-pyrenebutanoic acid, succinimidyl ester. Then, proteins formed an amide bond through the amino group, proteins were immobilized by anucleophilic substitution of N-hydroxysuccinimide (36).

Scheme 4

Noncovalent adsorption of SWCNTs with 1-pyrenebutanoic acid, succinimidyl ester via π–π stacking (68)

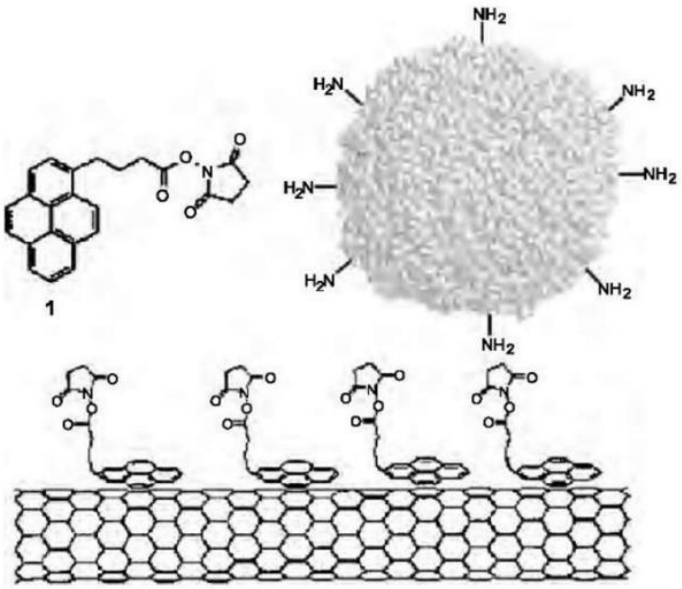

In another study, to increase the dispersion of multi-walled carbon nanotubes (MWCNTs), utilized functional polyesters, which have a number of functional groups (-OH, -COOH, and -CCH), to modify MWCNTs by stacking the pyrene functional polymer scaffold on top of the aromatic carbon nanotubes via π-π interaction. First, create a number of polyesters with alkyne moieties that lack electrons that enable Huisgen 1,3-cycloaddition processes to effectively introduce a variety of terminal functional groups, including pyrene, hydroxyl, carboxylic, and alkyne. Then, use pyrene-functional polyesters to interact non-covalently with the surface of MWCNTs via π-π stacking (figure 1.5). Because of the hydrophilic properties of the tetraethylene glycol and the terminal hydroxyl groups in the polyester's backbone, functionalized MWCNT well disperses in water (70).

Figure 1.5

structures of pyrene-functional polyesters. b) pyrene-functional polyesters interact non-covalently with the surface of MWCNTs via π-π stacking (70)

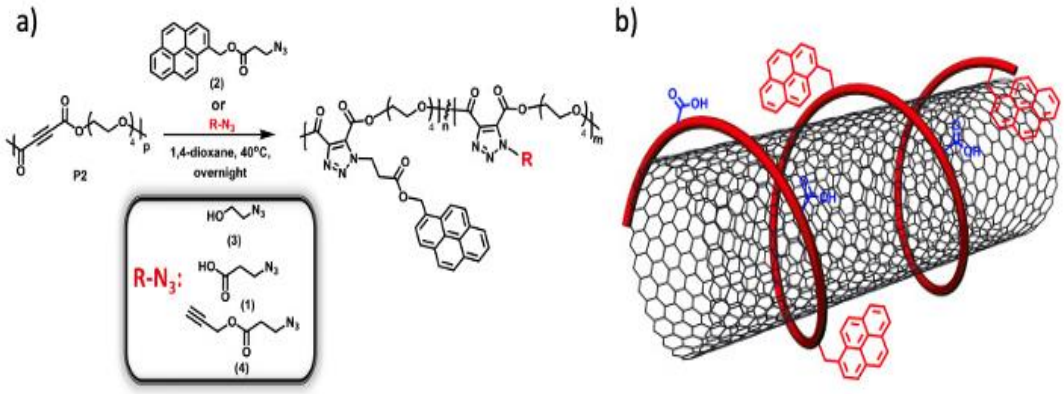

1.6 Chitosan

chitosan is a natural polyglucosamine (scheme 5), it has the benefits of being not toxic and biocompatible. Chitosan has been used in a variety of topical formulations, including hydrogels, powders, and dressings, which have all been studied in the wounds and burn animal models. Chitosan-containing products can enhance the re-epithelialization of wounds, collagen deposition, the proliferation of fibroblasts, and in general the healing wound's tensile strength (71).

Scheme 5

chemical structure of chitosan (72)

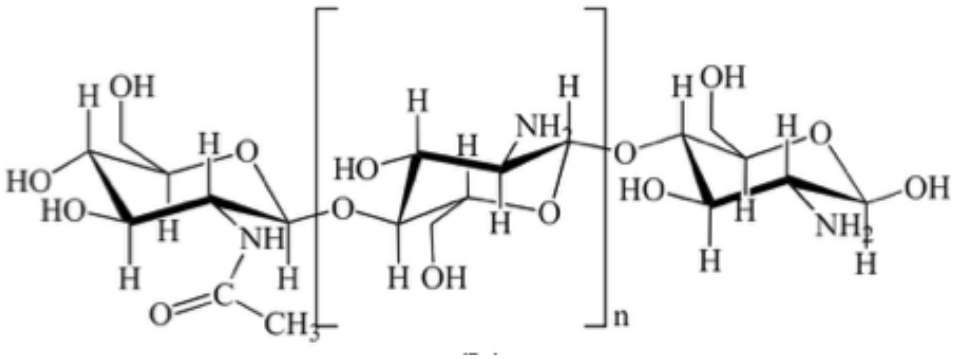

When administered chitosan to fresh wounds, it suppresses or reduces the number of fibroplasia. Chitosan has been shown to minimize exophytic callus in bone regeneration and allow vascular grafts to develop. It allows normal tissue elements to regenerate in skin lesions with minimum scar formation (73). Chitosan preparations increased the

histoarchitectural order and vascularization of the dermis layer, according to clinical investigations (74). SWCNTs and MWCNTs complexed with chitosan, via van der Waals interactions, so that the hydrophilic parts of the chitosan polymer would be exposed to the aqueous environment and wrap around the CNT, a hydrogel with a CNT scaffold was created. The addition of polar functional groups to CNTs may dramatically improve their dispersibility in aquatic settings and lower their toxicity, as a result, the hydrogel enhanced wound healing and re-epithelialization (75).

1.7 Literature Review

Several efforts were made to create suitable tissue engineering scaffolds using carbon nanomaterials, especially multi-walled carbon nanotubes. There are several reported approaches for utilizing MWCNTs to advance tissue engineering, which are presented in this literature review.

In 2011, Eri Hirata et al. prepared composite materials containing a rat primary osteoblast (ROBs), which were cultured on an MWCNT-coated collagen sponge (MWCNT-coated sponge) for bone tissue engineering, a surface coating treatment using MWCNTs was applied to a 3D collagen scaffold. MWCNT-coated sponges had considerably greater calcium and osteopontin concentrations than untreated sponges after 7 days. On the MWCNT-coated sponge, ROBs began to discriminate before they did on the uncoated sponge. Additionally, the tissue response to the MWCNT-coated sponge was evaluated. After implantation in subcutaneous tissue at 7 and 28 days, mild inflammation was seen surrounding MWCNTs. At 28- and 56-days following implantation in the femur, there was much more bone growth around the MWCNT-coated sponges than around the uncoated sponges, as well as new bone connected to MWCNTs directly. Furthermore, at 4 weeks after implantation bone tissues were successfully generated in the pores corresponding to the honeycomb structure of the MWCNT-coated sponge. As a result, MWCNT coating looks to be useful in the bone tissue engineering (76).

Mikael et al. in 2014 enhanced the mechanical strength of microsphere scaffolds of poly-lactic-co-glycolic acid (PLGA) by structuring them with carbon nanotubes, allowing them to be used for regeneration and load-bearing repair. They molded pristine and modified MWCNTs (with carboxylic acid (COOH) and hydroxyl (OH)) into 3-D

porous scaffolds to create PLGA microsphere scaffolds. The modulus and strength properties of pure PLGA scaffolds were dramatically boosted when only 3% MWCNTs were added. In the SEM picture, there was a significant difference in the distribution of MWCNTs on the surface of PLGA-MWCNTs scaffolds. While agglomeration was observed in all cases, modified MWCNTs had lower size agglomerates than non-modified MWCNTs, demonstrating the functionalized CNTs' dispersible nature (figure 1.6). As well cell adhesion and proliferation appeared to be perfect in SEM pictures. While tests on osteoblast-like MC3T3-E1 cells in vitro showed high cellular viability, proliferation, and mineralization. The *in vivo* investigation on 28 male rats showed differences in inflammatory response over the course of 12 weeks, with OH-MWCNTs having the lowest reaction and pristine MWCNTs and COOH-MWCNTs having a more prominent response. Overall, the results indicated that PLGA scaffolds including water-dispersed functionalized MWCNTs were mechanically stronger and had good tissue compatibility, indicating that they might be used in the bone tissue engineering (77).

Figure 1.6

MWCNT dispersion on the surface of PLGA-MWNT scaffolds as shown by SEM. The agglomeration size distribution within the unmodified MWCNTs is shown in red circle (77)

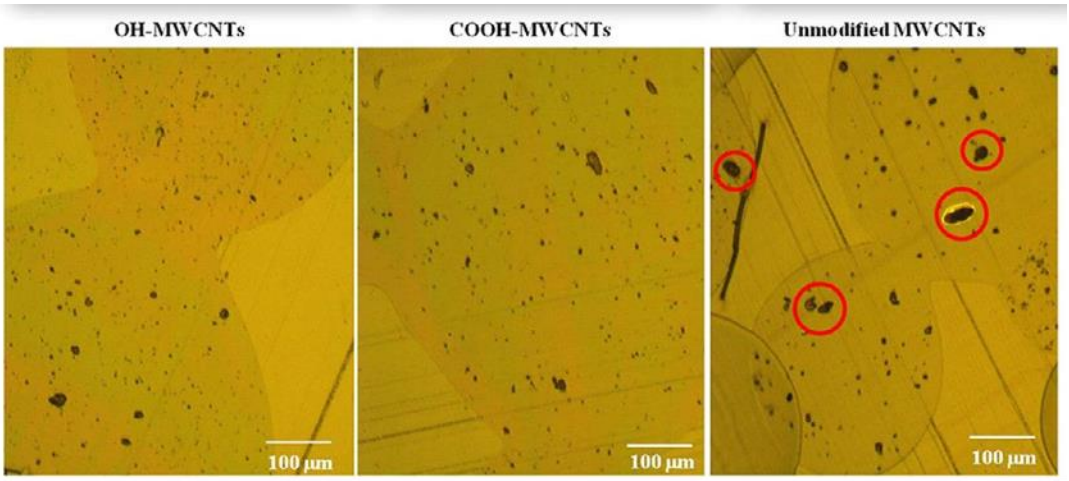

In another paper published a year later, researchers from Stony Brook University's Department of Biomedical Engineering reported on the fabrication and cytocompatibility of 3-D chemically cross-linked macro-sized porous CNTs scaffolds. The radical initiated thermal crosslinking of both SWCNTs and MWCNTs were used to create these scaffolds, and after 5 days, MC3T3 cells on SWCNTs and MWCNTs scaffolds had cell viability very well comparable to PLGA scaffolds because at day 3

and 5 there was no significant difference in total LDH release between the PLGA, MWCNT, and SWCNT scaffold groups. MC3T3 cells could connect and multiply SWCNTs and MWCNT scaffolds, as shown by immunofluorescence imaging and confocal live cell imaging. As a result, MC3T3 cells became round on low-surface-roughness scaffolds (SWCNTs) but elongated on high-surface-roughness scaffolds (MWCNTs). These findings showed that crosslinked SWCNTs and MWCNTs scaffolds are cytocompatible, opening the way for their development in tissue engineering applications (78)

in 2017, Shayan Gholizadeh et al. used chitosan and -Glycerophosphate with functionalized multi-walled carbon nanotubes, and the novel scaffold was prepared and characterized. according to in vitro experiments, increased f-MWCNT content improves electrical conductivity, but in the case of mechanical properties, The compressive strength of the samples was increased by increasing CNT content up to 0.1%, while compressive mechanical strength was slightly diminished by increasing CNT content up to 0.5%, and significantly degraded in mechanical strength by raising this value to 1%. Higher concentrations of CNTs can result in a significant increase in water uptake and porosity because they can increase the distances between chitosan chains and possibly break the chains' crosslinking (79). One year later, Valentina Martinelli et al. created an elastomeric scaffold made of microporous and self-standing polydimethylsiloxane (PDMS) material with micrometric voids, and they included multiwall carbon nanotubes (MWCNTs) in it. They used microscopy, cell biology, and calcium imaging to see if 3D-PDMS+MWCNT cultured neonatal rat ventricular myocytes (NRVMs) develop a more viable and mature phenotype than 3D-PDMS control. When compared to control PDMS, 3D-PDMS+MWCNT increased good cell proliferation while inhibiting cardiac fibroblast proliferation. 3D-PDMS+MWCNT can increase cardiac myocyte viability, proliferation, and functional maturation. These characteristics are critical in cardiac tissue engineering (80).

In 2021, Human foreskin fibroblasts (HFF-1) in collagen type I were used to make engineered connective tissues (ECTs), which were enriched with 3 different percentages of chitosan-coated MWCNTs (C-MWCNT); 0.025, 0.05, and 0.1 %. At whatever concentration, the used C-MWCNTs did not interfere with the embedding cells' alignment, and C-MWCNTs were distributed uniformly throughout the tissues. In

comparison to tissues without C-MWCNT, supplementation with 0.025% C-MWCNT increased tissue stiffness moderately but significantly. While adding 0.1% C-MWCNT to ECTs reduced tissue contraction and improved extensibility, elasticity, and biomechanical properties, This could be used for future in vivo connective tissue repair applications, such as the dermis layer in the skin, ligaments, and tendons, which demand strong tolerance capacities against external stressors. Regardless of the condition, C-MWCNT supplementation could improve the biophysical properties of ECTs, which could be beneficial for connective tissue repair applications (81).

In another study, the electrospinning method was used to create polyurethane nanofiber with varying concentrations of gelatin and SWNT. Gelatin and SWNTs were combined to reduce the mean diameter of nanofibrous scaffolds from 210 to 140 nm, which had an effect on the initial behavior of the cells. It was discovered that nanofibrous scaffolds' hydrophilicity significantly increased after gelatin and SWNTs were added. Gelatin was used to modify the scaffold degradation profile. The scaffolds' electrical conductivity was significantly improved by the addition of SWNTs. After 7 days of culture, biological evaluation by SEM and MTT assay showed that the nanofibrous surface was covered by a dense layer of confluent endothelial cells and myocardial myoblast, which is essential for cardiovascular tissue engineering. The results demonstrated the potential of the manufactured scaffolds for the cardiovascular tissue engineering (82).

Previous literature has shown that conductive materials, such as carbon nanomaterials (83), stimulate the proliferation and differentiation of electrical stimulus-responsive cells such as muscle cells (84, 85), neuron cells (86-88), bone cells (89, 90). Carbon nanotubes, a conductive material, are used to achieve the functional differentiation of transplanted cells in tissue engineering by mimicking the properties of the microenvironment, they stimulate stem cells to differentiate into electroactive lineages, emphasizing the potential involvement of stem cells in electroactive tissue regeneration (e.g. nerve and heart) (91-93).

Our previous works, started by functionalizing the CNTs non-covalently based on pyrene derivatives and studying their suitability as a scaffold for the tissue engineering (94). In this work, we will construct a connective tissue based on primary cells extracted from mice skin and continue to test collagen hydrogel that is fortified by MWCNTs,

which are noncovalently functionalization with pyrene moiety and coated with chitosan as a scaffold for connective engineering.

1.8 Aims of the study

The main aim of this project is to utilize the previously functionalized MWCNTs terminated with COOH or amine group in our research group to develop a scaffold for connective tissue based on primary cells extracted from mice skin, and decorted with chitosan to achieve enhanced electrical conductivity and acceptable biocompatibility as shown in figure A.1 (in appendix A).

1.9 Objectives

1. Synthesize the pyrene derivatives terminated with carboxyl or amine groups that have been previously developed in our group for the effective functionalization of the MWCNTs.
2. Non-covalently functionalization of the MWCNTs and also decort them with chitosan.
3. Characterization of the developed nanocomposites
4. Assess the electrical properties of the formed engineered tissue
5. Assess the biocompatibility of the engineered tissue.

Chapter Two

Methodology

2.1 Reagents and instrumentation

tetraethylene glycol (TEG) (Catalog # B23990), propargyl bromide (Catalog # A16580), EDC (catalog # A10807), 1-Pyrenebutyric acid (Catalog # A17760) and L-ascorbic acid sodium salt (Catalog # A17759) were obtained from (Alfa Aesar company in England). MWCNTs were obtained from (Nanostructured and Amorphous Materials, USA). We obtained Sodium azide (NaN) (Catalog # 0E30428) from Germany (RiedeldeHaën Company). Methanol (MeOH), Aceton, dichloromethane (DCM), ethanol (EtOH), and isopropyl alcohol were obtained from (Haifa C.S. Company,). Diethyl ether (catalog # 38132) and triethylamine (Et3N) (Catalog # 40502L05) were obtained from (Merck Millipore). 4-(dimethylamino) pyridine (DMAP) (Catalog # 1122583) and anhydrous copper sulfate (Catalog # 451657) were obtained from (Sigma-Aldrich, USA). n-hexane (Hex) (Catalog # 2355544800024) and ethyl acetate (EtOAc) (Catalog # 2355516100024) solvents were obtained from (Frutarom Company, Haifa). While Tetrahydrofuran (THF) solvent (Catalog # 487308) was obtained from (Carlo Erba Company, Italy).

Purification of the products using column chromatography with silica gel (pore size 60) from the Sigma Aldrich Company. Water bath sonicators were used in the dispersion and preparation of functionalized MWCNTs (MRC DC-200H Digital Ultrasonic Cleaner) and centrifuges (UNIVERSAL 320, Hettich Zentrifugen, Germany). A rotary evaporator (MRC, ROVA-100, laboratory equipment company) was employed to dry the solvents. TLC was used to monitor the reactions (DC-Fertigfolien ALUGERAM®SIL G/UV254, MACHEREY NAGEL Company, Germany).

For biological tests utilized Penicillin/streptomycin solution (pen/strep) (REF #03-031-1B), phosphate-buffered saline (PBS, Ca+2 free), and high glucose Dulbecco's Modified Eagle Medium (DMEM) from (Biological Industries, Jerusalem). Fetal Bovine Serum (catalog # F7524), DMEM powder (Catalog # 56436C-10L), Trypsin-EDTA solution 1X (Catalog # 59417C), L-Glutamine solutions (Catalog #G7513), Chitosan powder (CAS 912_76_4) and bovine skin collagen solution (Catalog # C4243-20ML) were obtained from Sigma-Aldrich, USA.

Pipetting was done using variable Accumax Micropipette (made in the UK), incubating the cell line was done in an Esco cell culture CO_2 incubator. In the cell viability test, To scan the plate, a Unilab Microplate Reader 6000 was employed. Vector Network Analyzer (made in Switzerland) was used to measure electrical conductivity, Digital microscope, and Leica ICC50 HD used to obtain digital images.

2.2 Synthesis of pyrene derivatives

The pyrene-COOH was synthesized according to our previously published work (94). Regarding the pyrene-NH2 has been synthesized as follows:

2.2.1 Tosyl-TEG-Tosyl Synthesis (1)

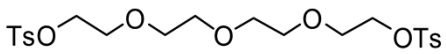

Tetra ethylene glycol (TEG) (4g, 20.59 mmol), triethylamine (Et_3N) (9.23ml, 51.25 mmol) were dissolved in 40 ml Tetrahydrofuran (THF) and stirred for five minutes, the reaction then cooled in an ice bath, and tosyl chloride (10 g, 51.25 mmol) was added gradually to the mixture. At room temperature and overnight the reaction was stirred. The product was diluted by dichloromethane (DCM) (100ml) and 1 M Hydrochloride (HCl) (50 ml). 100 ml of DCM was used to wash the aqueous layer. After that, sodium sulfate (Na2SO4) was used to dry the collected organic layers, and then evaporated the excess solvent under vacuum and obtained a mixture product of (11.3 g). the product was purified using silica column chromatography in a 1:1 Hexane/Ethyl acetate to get a product that is oily yellow and has a yield of (5.92 g, 24.24 mmol, 52.4%)

R_f : 0.42 (Hexane/Ethyl acetate (1:1)).

^{1}H NMR: (500 MHz, $CDCl_3$): δ7.76 (d, 4H, *J* = 8.2 Hz, Ts), 7.30 (d, 4H, *J* = 7.8 Hz, Ts), 4.11 (t, 4H, *J* = 4.6 Hz, $2CH_2OTs$), 3.63 (t, 4H, J = 4.6 Hz, $2OC\underline{H_2}CH_2OTs$), 3.54-3.50 (m, 8H, $4CH_2O$), 2.40 (s, 6H, $2CH_3$).

^{13}C NMR (125.7 MHz, $CDCl_3$): δ 144.9, 133.0, 129.9, 128.0, 70.7, 70.5, 69.3, 68.7, 21.6.

2.2.2 N_3-TEG-N_3 Synthesis (2)

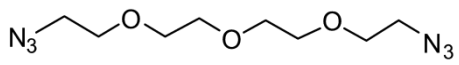

Compound (1) (1.2g , 4.912 mmol) was added to a 100 ml round bottom flask (RBF) and was dissolved by 10 ml Ethanol. Then sodium azide (798.5mg, 12.28mmol) was added to the solution, the reaction was stirred in reflux at 70 ºC overnight. The product was diluted using diethyl ether (100 ml) and saturated sodium chloride (NaCl) (50 ml). 100 ml of diethyl ether was used to wash the aqueous layer. After that, sodium sulfate was used to dry the obtained organic layers (Na2SO4), and the excess solvent was evaporated under vacuum. The obtained yield was (0.6195 g, 2.538 mmol).

R_f: 0.625 (Ethyl acetate/Hexane (2:1))

^{1}H NMR: (500 MHz, $CDCl_3$): δ 3.62-3.60 (m, 8H, $4CH_2O$), 3.33 (t, 4H, *J* = 5.0 Hz, $2OC\underline{H_2}CH_2N_3$), 2.56 (t, 4H, *J* = 4.5 Hz, $2CH_2N_3$).

^{13}C NMR (125.7 MHz, $CDCl_3$): δ70.7, 70.0, 50.7, 40.9.

2.2.3 OH-TEG-alkyne Synthesis (3)

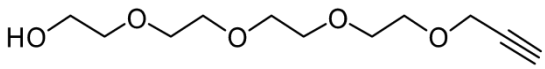

In 100 ml Round bottom flask, 3 g of TEG (15.4 mmol) was added and dried under vacuum and then dissolved in 20 ml of anhydrous THF under argon. A dried solution of sodium hydride (NaH) (741 mg, 30.9 mmol) and anhydrous THF (10 ml) were added drop by drop to the TEG solution until the release of Hydrogen gas (H_2). After 30 min, Anhydrous THF (10 ml) was mixed in a dry solution of propargyl bromide (1.9 ml, 21.6 mmol) and added to the reaction. The reaction was continuously and vigorously stirred at room temperature overnight. The following day, drop by drop added of 5 ml of water to the reaction, and THF was evaporated. DCM (100 ml) and HCl (50 ml) were used to dilute the crude product then it was dried with Na2SO4., filtered and evaporated, the crude product was (2.3462g). Silica column chromatography in ethyl acetate was used to purify the product to produce a product that is oily yellow and has a yield of (1.2742 g, 5.49 mmol, 54.31%).

R_f: 0.3714 (Ethyl acetate).

^{1}H NMR(500 MHz, $CDCl_3$): δ 4.24 (d, 2H, J = 2.9 Hz, CH_2C), 3.65–3.58 (m, 14H, $7CH_2O$), 3.57–3.51 (m, 2H), 2.95 (s, 1H, CH), 1.1 (s, 1H, OH). **^{13}C NMR (125.7 MHz, $CDCl_3$):** δ 92.6, 78.8, 74.5, 72.3, 70.8, 70.7, 70.7, 70.6, 70.3, 69.1, 61.5, 58.4.

2.2.4 Pyrene-TEG-alkyne Synthesis (4)

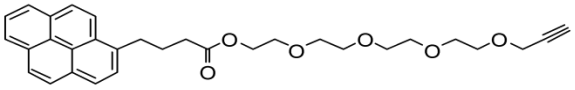

Compound (3) (1 g, 4.3 mmol), 620.7 mg of pyrenebutyric acid (2.2 mmol), 1.2 g of EDC (6.5 mmol) and 396.2 mg of 4-Dimethylaminopyridine (DMAP) (3.2 mmol) were dissolved in 20 ml DCM and were reacted under argon. For 24 hours, the reaction was stirred continuously at room temperature. The resulting product was dried with Na2SO after being collected using DCM (170 mL) and 1 M HCL (50 mL), filtered and evaporated. the product was purified using silica column chromatography in a 3:2 mixture of ethyl acetate/n-hexane to produce a product that is oily yellow and has a yield of (916 mg, 1.7 mmol, 41.3%).

R*f*: 0.3 (Ethyl acetate/n-Hexane (2:3)).

^{1}H NMR: (500 MHz, $CDCl_3$): δ8.29-7.83 (m, 9H,Py), 4.23 (s, 2H, CH_2OCO), 4.15 (s, 2H, $OCH_2C{\equiv}CH$), 3.67-3.53 (m, 14H, $7CH_2O$), 3.37 (t, 2H, J = 7.2 Hz, Py-CH_2), 2.47 (t, 2H, J = 7.2 Hz, CH_2COO), 2.39 (s, 1H, C≡CH), 2.20-2.15 (quint, 2H, Py-CH_2CH_2).

^{13}C NMR (125.7 MHz, $CDCl_3$): δ173.5, 135.8,131.4, 130.9, 130.0, 128.7, 127.5, 127.4, 126.7, 125.9, 125.1, 125.0, 124.9. 124.8, 123.4, 72.5, 70.5, 70.4, 70.2, 69.7, 69.2, 69.1, 64.6, 63.5, 61.6, 61.5, 61.0, 33.8, 32.7, 29.7, 26.8.

2.2.5 Pyrene-TEG-triazole-TEG-azide Synthesis (5)

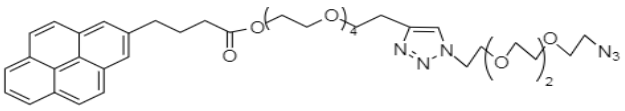

compound (4) (350 mg, 0.69mmol) and Compound (2) (200 mg, 0.82 mmol) were dissolved in DCM (3ml), and a solution of sodium ascorbate (62.1mg, 0.313mmol), and anhydrous copper sulfate (22.23mg, 1.4mmol) in H_2O (3ml) was added. The reaction was stirred for twenty-four hours at room temperature. The product was first diluted with DCM (100 ml) and water (50 ml), dried with Na2SO4, filtered, and evaporated. Then the product was purified using silica column chromatography in 20:1 mixture of DCM/MeOH, to produce a product that is oily yellow and has a yield of (192mg, 0.25mmol. 54%).

R*f*: 0.33 (DCM/MeOH (20:1)).

^{1}H NMR: (500 MHz, $CDCl_3$): δ 8.27 (d, 1H, *J* = 9.2 Hz, Py), 8.13 (dd, 2H, *J* = 6.9 Hz, *J* = 5.5 Hz, Py), 8.08 (dd, 2H, *J* = 3.7 Hz, *J* = 2.3 Hz, Py), 8.00-7.93 (m, 3H. Py), 7.83 (d, 1H, J = 7.8 Hz, Py), 7.74 (bs, 1H, CH triazole), 4.62 (s, 2H, CH_2-triazole),4.46 (t, 2H, *J* = 5.0 Hz, CH_2OCO), 4.21 (t, 2H, *J* = 4.8 Hz, CH_2N-triazole), 3.79 (t, 2H, *J* = 5.0 Hz, $C\underline{H_2}CH_2N$-triazole), 3.65-3.53 (m,26H, $13CH_2O$),3.36-3.30(m, 4H, CH_2CO, CH_2N_3), 2.45 (t, 2H, *J* = 7.3 Hz, Py-CH_2), 2.15 (quint, 2H, Py-$CH_2C\underline{H_2}$).

^{13}C NMR (125.7 MHz, $CDCl_3$): δ173.5, 135.8, 131.4, 130.9, 130.0, 128.7, 127.5, 127.4, 126.7, 125.9, 125.0, 124.9, 124.8, 123.4, 70.7, 70.6, 70.5, 70.0, 69.7, 69.4, 69.2, 64.5, 63.5, 50.7, 33.8, 32.7, 26.8.

2.2.6 pyrene-TEG-triazole-TEG-amine Synthesis (6)

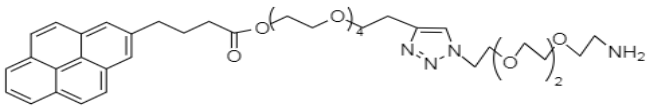

Compound (5)(90 mg, 0.118 mmol) and palladium on carbon (9 mg) (as a catalyst) were dissolved in 5 ml methanol under hydrogen. For twenty-four hours and at room temperature, the reaction was stirred. The product was extracted by 100 ml of DCM,

3ml of methanol, and evaporated, before being filtered and rewashed with Mmethanol then re-evaporated. The obtained yield was 93 mg.

^{1}H NMR: (500 MHz, $CDCl_3$): δ8.36 (d, 1H, *J* = 11.0 Hz, Py), 8.24-7.96 (m, 8H, Py), 7.90 (s, 1H, CH triazole),4.47-4.44 (m, 4H, CH_2-triazole, NH_2),4.31 (t, 2H, *J* = 4.6 Hz, CH_2OCO), 4.11 (t, 2H, *J* = 5.0 Hz, CH_2N-triazole), 3.78-3.73 (m, 2H, $C\underline{H_2}CH_2N$-triazole), 3.55-3.35 (m, 30H, $13CH_2O$, CH_2CO, $C\underline{H_2}NH_2$), 2.44-2.42 (m, 2H, Py-CH_2), 2.12 (quint, 2H, Py-$CH_2C\underline{H_2}$).

^{13}C NMR (125.7 MHz, $CDCl_3$): δ173.3, 144.3, 136.7, 131.4, 130.9, 129.9, 128.6, 127.9, 127.8, 127.0, 126.6, 125.4, 125.3, 124.7, 124.63, 123.9, 72.8, 70.2, 70.1, 70.0, 69.4, 69.2, 68.8, 64.0, 63.6, 60.7, 56.5, 49.8, 33.6, 33.4, 32.3, 29.5, 27.3, 27.2.

2.2.7 OH-TEG-Tosyl synthesis (7)

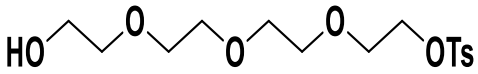

The compound was synthesized and identified as in the literature (95) .

2.2.8 OH-TEG-N_3 Synthesis (8)

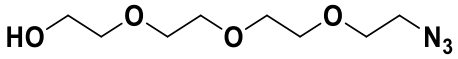

The compound was synthesized and identified as in the literature (96).

2.2.9 COOH-TEG-N_3 synthesis (9)

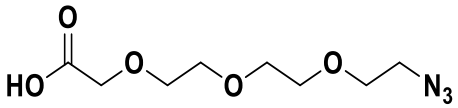

The compound was synthesized and identified as in the literature (96).

2.2.10 Pyrene-TEG-triazole-TEG-COOH Synthesis (10)

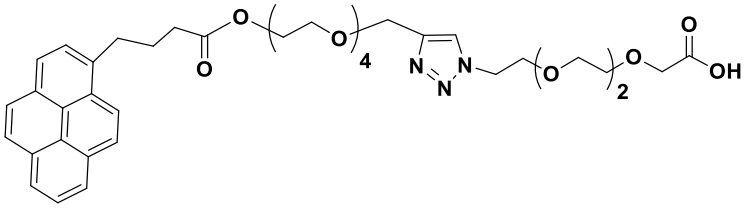

The compound was synthesized and identified as in the literature (97).

2.3 Optimizing the needed amount of compound (6) or (10) to functionalize MWCNTs in water

Compounds (6) or (10) in varying concentrations (0.25, 0.5, and 1 mg) were dissolved in 1 mL of water before being mixed with 1 mL of MWCNTs and sonicated for 30 minutes. The various dispersions were then kept under observation so that the best concentration could be determined for dispersing carbon nanomaterials in water without precipitation or an excess of micellar structures visible in TEM images.

2.4 Functionalization of MWCNTs with Py-COOH and Py-NH2

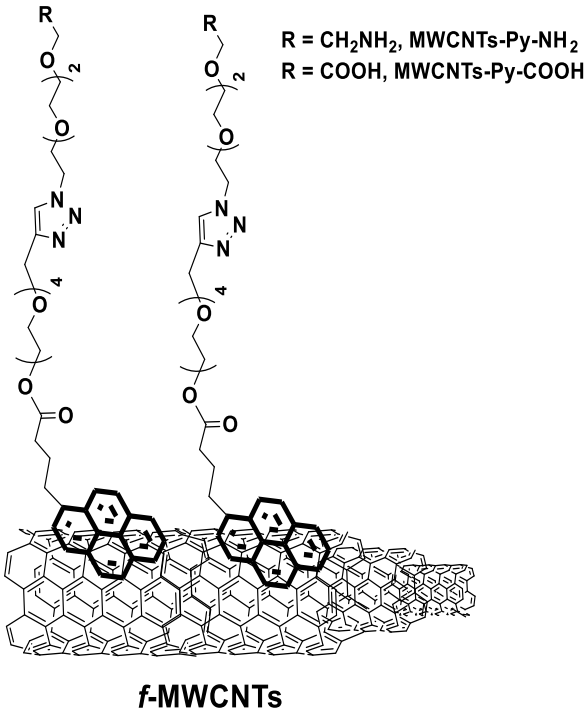

Optimum amount of Py-COOH and Py-NH2 were dissolved in H_2O (1 mL) then 1 mL of MWCNTs were added up to the solution and the mixture was sonicated for 30 minutes. The products were then dried by a freeze-dryer.

2.5 Atomic force microscope characterization

The morphology and diameters of the unfunctionalized and functionalized multiwalled carbon nanotubes were determined using an atomic force microscope (CoreAFM, nanosurf, Switzerland) using the tape mode and the cantilever (Dyn190Al with Resonant frequency = 190 kHz).

2.6 Primary dermal fibroblast culture and maintenance

- **Preparation of fibroblast growth medium with 20% FBS**

A bottle of 500 ml of high glucose DMEM was supplied with 100 ml fetal bovine serum (FBS), 5ml penicillin/streptomycin, and 5ml L- glutamine.

- **Isolation and culturing of primary dermal neonatal mouse fibroblasts**

Neonatal mice were euthanized by cervical dislocation. After being sterilized with 70% ethyl alcohol followed by a povidone-iodine solution, the limbs and the tails of the mice were cut off before the skin was taken off. The skin was then washed twice with PBS under a sterile laminar flow. After that, the skin was transferred to a 100 mm petri dish and by using surgical scissors it was cut into small pieces of about 2-3 mm^2. Then, the tissue pieces were transferred to a flacon tube containing 5ml 0.25%trypsin solution and were incubated at 37^oC for 15 minutes. Every 5 minutes the falcon tubes were shaken gently and 5 ml of 0.25% fresh trypsin solution was added to each one. After that, a sufficient fresh culture medium containing 20% FCS was added to each tube to inactivate the trypsin. Then the tissue pieces were transferred to 6-well plates with the dermis layer facing downwards. The tissues were left to partially dry under the laminar flow until they stuck to the plastic surface, then approximately 700 microliters medium were added carefully.

The tissue culture plates were incubator at 37°C with 5% CO2 to allow the outgrowth of the cells from the tissue pieces. Every other day the medium was changed until the cells were about 90% confluent.

2.7 Generation of Engineered Connective Tissue (ECT) with/without functionalized MWCNT

2.7.1 Double-strength cell culture media (2x DMEM) preparation

To create a medium with double strength, 267. 2 mg DMEM powder (13.36g/L), 74 mg of NaHCO3 (3.7g/L), and 2 ml of FBS were added to 18 ml of the ready-to-use1x DMEM. The mixture was stirred for 30 minutes before sterile filtering with a 0.22-micrometer syringe filter.

2.7.2 Preparation of 0.1% NaOH

Forty mg of sodium hydroxide (NaOH) was dissolved in 10 mL of distilled water and was then filtered through a 0.22-micrometer syringe filter.

2.7.3 Preparation of 1.5 % (W/V) chitosan

By combining 20 ml of 1% (v/v) acetic acid with 300 mg of chitosan. The mixture was sonicated for 1 hour to completely dissolve chitosan.

2.7.4 Primary cell suspension preparation

First, the cells were washed twice with Ca^{+2}-free PBS after the old medium was removed. After that, 0.05 percent trypsin was added to the cells just enough to cover them, and the plate was left in the cell culture incubator at 37 °C and 5% CO2 for up to 5 minutes. The cells were examined under the microscope continually until most cells detached from the flask. A sufficient amount of DMEM growth medium (containing 20% FCS) was added to inactivate the trypsin. The cell suspension was collected in a 50 ml falcon tube, and the cell concentration was determined by a cell counting chamber. The cells were then centrifuged at 200 RCF for 7 minutes at 4^{o}C. The supernatant was removed and the cell pellet was resuspended in a fresh growth DMEM medium to obtain the desired cell concentration (7.5×10^{6} cell/ml).

2.7.5 Preparation of MWCNTs-NH2 and MWCNTs-COOH Stock solutions

Fifty mg of each f-MWCNTs species was mixed with 1200 microliters of PBS to obtain a 4% (w/v) of f-MWCNTs suspension. The mixture was sonicated for at least 120 min to enhance the dispersion of f-MWCNTs. After that, the suspension was autoclaved in a humidified environment.

2.7.6 Preparation of engineered connective tissues (ECTs)

The ECTs were formulated according to a method described by Kittana et al., 2021(81). Table 1 presents the formula of a single ECT (about 255 μL volume) without the addition of any type of f-MWCNTs.

All of the used materials in this experiment were maintained at 4°C and kept cold during the experiments. Here the ECTs were prepared by mixing collagen (3 mg/mL), 2x DMEM, and PBS. The pH was then titrated to neutralization with 0.1 N NaOH until the liquid became pink in color. The cell suspension (containing the required cell number per ECT) was then added to the Eppendorf, and the mixture was pipetted immediately in the form of a ring around a pair of flexible poles fitted in a special model of 48-well mold plate (Myriamed, Göttingen, Germany) (figure A.2 in appendix A). The plate was then transferred to the incubator (37°C, 5% CO2) for 45 minutes. A fresh DMEM growth medium was added at this step, and the plate was placed in the incubator for 5 days, with the medium being changed every other day. The formula was scaled up based on the number of ECTs to be prepared.

Table 1

ECT general composition

Constituent	Volume (μL)
Collagen	100
2x DMEM	100
PBS	6.4
NaOH (0.1 N)	~ 5
Cell suspension (7.5×10^6 cell/mL).	44
Total	~ 255.4

2.7.6.1 Preparation of f-MWCNTs containing ECT

- **ECT containing F-MWCNT**

The various ECTs containing different types of f-MWCNTs were prepared using the same methodology as before, but instead of PBS, we used an equivalent volume of a stock solution containing enough CNTs to obtain the target total concentration in the ECT master mix. Tables 2, 3, and 4 contain the formula for a single ECT containing 0.025%,0.05%, and 0.1% f-MWCNT (either MWCNT-NH2 or MWCNT-COOH), And the formula was scaled up based on the number of ECTs to be prepared.

Table 2

ECT contains 0.025% f-MWCNT general composition

Constituent	Volume (μL)
Collagen	100
2x DMEM	100
4% f-MWCNT	1.6
PBS	4.8
NaOH (0.1 N)	~ 5
Cell suspension (7.5 x 10^6 cell/mL).	44
Total	~ 255.4

Table 3

ECT contains 0.05% f-MWCNT general composition

Constituent	Volume (μL)
Collagen	100
2x DMEM	100
4% f-MWCNT	3.06
PBS	3.34
NaOH (0.1 N)	~ 5
Cell suspension (7.5 x 10^6 cell/mL).	44
Total	~ 255.4

Table 4

ECT contains 0.1% f-MWCNT general composition

Constituent	Volume (μL)
Collagen	100
2x DMEM	100
4% f-MWCNT	6.4
NaOH (0.1 N)	~ 5
Cell suspension (7.5×10^6 cell/mL).	44
Total	~ 255.4

2.7.6.2 preparation of chitosan and f-MWCNTs containing ECT

- **Chitosan containing ECT (control)**

The ECTs were prepared as described earlier, except that chitosan solution was included in the formula at the expense of the collagen proportion (Table 5).

Table 5

General composition of chitosan-containing ECT

Constituent	Volume (μL)
Collagen	50
Chitosan	50
2x DMEM	100
NaOH (0.1 N)	~ 50
Cell suspension (7.5×10^6 cell/mL).	33
Total	~ 283

- **Chitosan and 0.025% MWCNT-COOH containing ECT**

Table 6

chitosan and 0.025%MWCNT-COOH containing ECT

Constituent	Volume (μL)
Collagen	50
Chitosan	50
2x DMEM	100
4% MWCNT-COOH	1.83
NaOH (0.1 N)	~ 50
Cell suspension (7.5×10^6 cell/mL).	33
Total	~ 284

2.8 Characterization of Engineered Connective tissues

2.8.1 Electrical conductivity of ECTs

After DMEM growth medium removal, PBS was used to wash the tissue samples, then the electrical conductivity was measured by Vector Network Analyzer which provides high-precision measurements of dielectric parameters (conductivity, permittivity, loss tangent) over an extremely broad frequency range from 200 MHz to 14 GHz, the probe is coupled to a vector network analyzer (VNA) to measure the complex reflection coefficient at the probe end.

2.8.2 Cell viability test (MTS assay)

2.8.2.1 Preparation of the treatment solution for MTS assay

Medium samples containing different concentrations of the tested compounds were prepared to use for MTS assay, preparation of medium solutions containing 0.025%, 0.05%, and 0.1% MWCNT-COOH, Chitosan solution (add 300 μL chitosan to 1100 μL medium and neutralized the mixture with approximately 360 μL NaOH), 0.025% MWCNTs with Chitosan solutions, and 0.025%,0.05% and 0.1% Pyrene-COOH solutions.

2.8.2.2 Cell culture

Primary fibroblasts were cultured in DMEM growth media and incubated at 37˚c with 5% CO2. The cells were collected by trypsinization as mentioned above when they were around 80-90 percent confluent. The concentration of the cell suspension was adjusted to 100,000 cells/mL. A 96-well plate was then filled with the cell suspension, as 100 microliters per well, so that each well receives 10,000 cells. Some wells did not receive cells to serve as blank samples. The cells were left to adhere and adapt for 48 hours before starting the treatment.

2.8.2.3 MTS assay

After primary fibroblast cells were sub-cultured and left for 48 hours to adhere and accommodate in a 96-well plate, the DMEM growth medium was replaced by 100 uL of a treatment solution. Control wells and blank wells received fresh DMEM growth medium. The cells were incubated for 24 hours with the treatment conditions. After that, the treatment conditions were replaced by a 100 uL fresh DMEM growth medium containing 10% MTS reagent, and the plate was put in the incubator at 37 °C and 5% CO2. After one hour, a microplate reader was used to measure the absorbance at 492 nm.

Chapter Three

Results and Discussion

3.1 Synthesis and functionalization of carbon nanomaterials

This project aimed to non-covalently functionalize carbon nanotubes such that the electrical properties of the carbon nanostructure can be preserved to generate an electrically conductive scaffold for tissue engineering. We achieved this by using the pyrene moiety to interact with the MWCNT surface via π-π stacking. In addition, the pyrene moiety was linked to a hydrophilic linker to provide an appropriate hydrophobic/hydrophilic ratio capable of dispersing carbon nanotubes in water.

We synthesized two hydrophilic linkers COOH-TEG-N_3 and NH2-TEG-N_3 which were reacted with Py-TEG-alkyne through click reaction. Forming Py-TEG-triazole-TEG-COOH or Py-TEG-triazole-TEG-NH_2. We choose two hydrophilic linkers that terminated with a carboxyl or amine group to study if this terminated group has an effect on the electrical property or in the formation of the constructed tissue. The synthesis began by reacting the tetraethylene glycol with propargyl bromide to form the terminal alkyne linker which reacted with pyrene butyric acid to from pyrene terminal alkyne as shown in Scheme 6.

Scheme 6

The synthesized OH-TEG-alkyne linker (1) was reacted with pyrene butyric acid to obtain Py-TEG-alkyne (2)

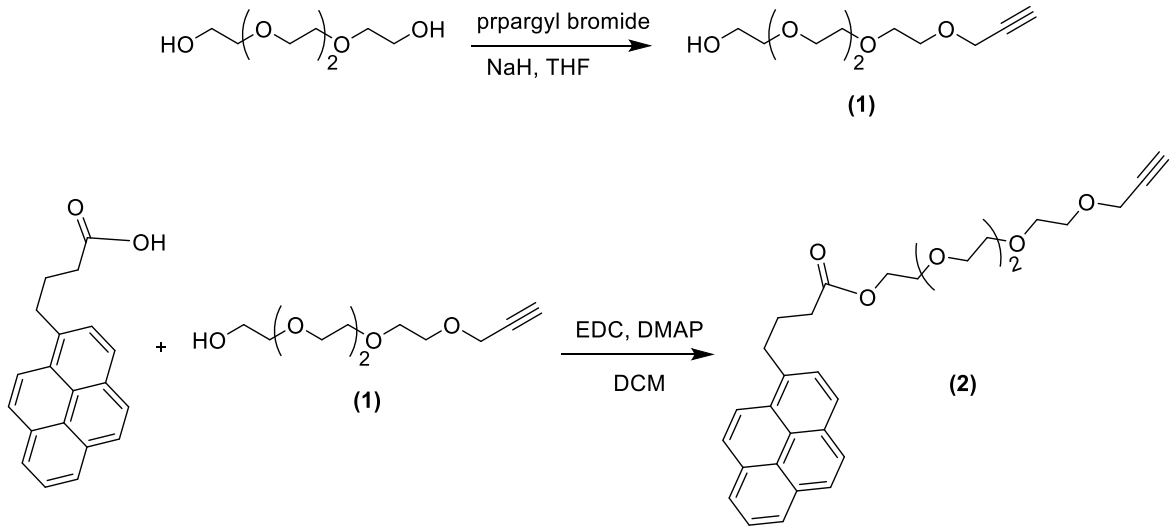

After that, two hydrophilic derivatives of tetraethylene glycol were synthesized to react with the pyrene moiety to have a terminal cabroxyl or amine group. In order to synthesize the TEG-COOH, The tetraethylene glycol was reacted with 1 equivalent of tosyl chloride followed by the conversion to azide by reacting with sodium azide. Then a final oxidation step using Jones reagent to form compound 5 (COOH-TEG-N3). Finally, compound 5 was reacted with pyrene-alkyne 2 using click reaction to obtain the final product compound 8 as shown in scheme 6.

To synthesize the terminal amine group, the tetraethylene glycol was reacted with two equivalents of tosyl chloride to obtain the ditosylated linker which was converted to diazide using two equiavlents of sodium azide to synthesize compound 7. After that compound 7 was reacted with pyrene-alkyne 2 using a click reaction followed by a reduction reaction to obtain the final compound 9 as shown in Scheme 7.

Scheme 7

*Synthesis of Py-TEG-triazole-TEG-COOH **(8)** and Py-TEG-triazole-TEG-NH2 (9)*

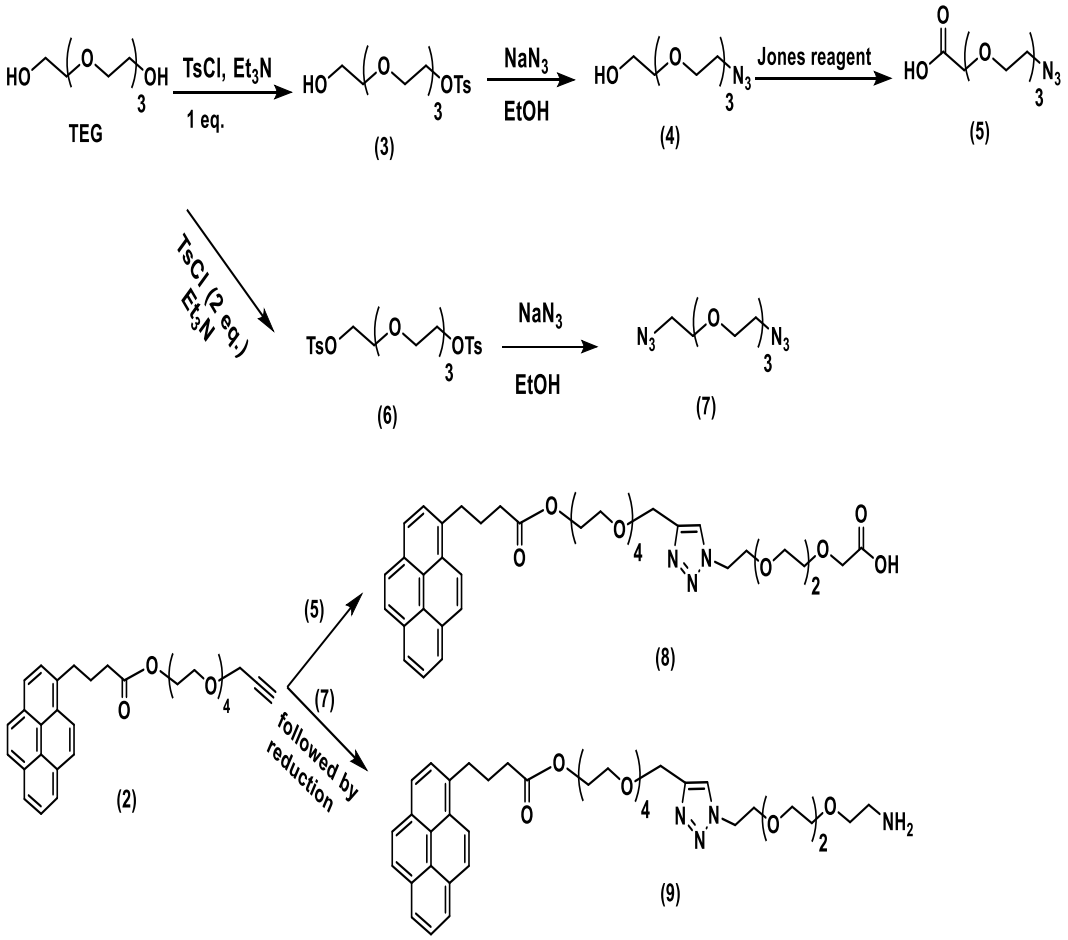

After the successful synthesis of the two pyrene derivatives, they were utilized to functionalize the MWCNTs non-covalently. It has been found that the needed amount from compound 8 or 9 to disperse the MWCNTs is 0.5 mg/ml where the pristine MWCNTs form aggregates and precipitate immediately whereas the functionalized MWCNTs with py-COOH or Py-NH_2 showed good water dispersibility and stability as shown in figure 3.1.

After the dispersion and the functionalization of the MWCNTs, an atomic force microscope (AFM) was conducted to evaluate the morphology and dispersibility of the MWCNTs. As can be observed in figure 3.2, the pristine MWCNTs showed the formation of a huge mesh of carbon nanotubes due to the hydrophobic interaction between the walls of the nanotubes. However, upon the non-covalent functionalization with the pyrene derivatives the carbon nanotubes become dispersed in water due to the

introduction of the hydrophilic groups as can observe in Figure 3.2 B and C, we noticed the separation of the nanotubes and we can see single multiwalled carbon nanotubes with diameter ranges between 20 and 30 nm. These images confirm the successful functionalization of the carbon nanotubes with the successful separation of the nanotubes.

Figure 3.1

Image of dispersion of A) pristine MWCNTs; B) MWCNTs-Py-COOH and (C) MWCNTs-Py-NH2

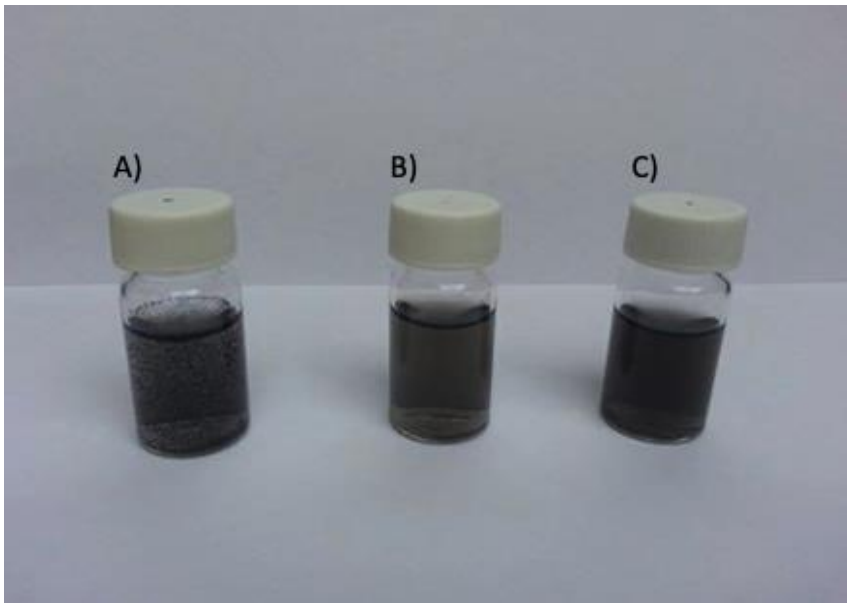

Figure 3.2

A) pristine MWCNTs, B) f-MWCNTs with py-COOH, C) f-MWCNTs with py-NH_2

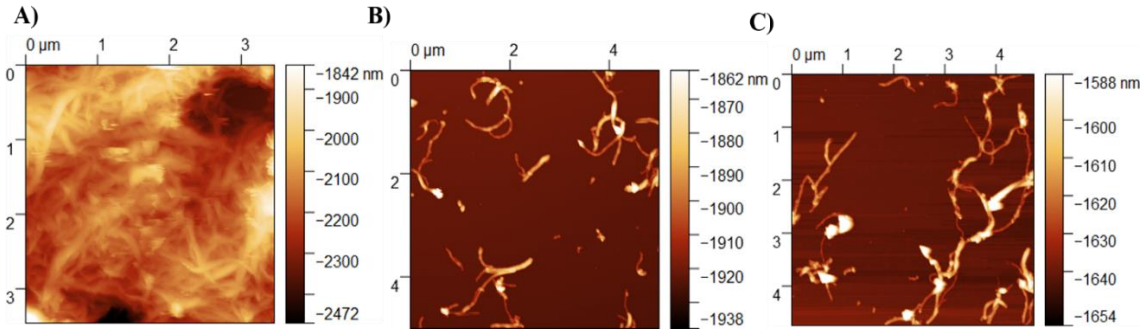

3.2 Casting and characterization of connective tissues

3.2.1 ECTs Generation with primary dermal fibroblast

With varying kinds and concentrations of f-MWCNTs, ECTs including primary dermal fibroblast cells were created (figure 3.3). The control tissues were whitish, opaque, and cohesive ring around stretchers, As expected, the addition of f-MWCNTs changed the tissue's color into dark gray-black, depending on the concentration of f-MWCNTs. Over 5 days of incubation, the tissues condensed in the form of a ring and contracted the stretchers. At this point, the tissues were mature enough to undergo the conductivity test.

Figure 3.3

primary fibroblast-containing ECT with varying MWCNTs loading: A) Control; B) MWCNTs-Py-COOH (0.025%); C) MWCNTs-Py-COOH (0.05%); D) MWCNTs-Py-COOH (0.10%); E) MWCNTs-Py-NH2 (0.025%); F) MWCNTs-Py-NH2 (0.05%) and G) MWCNTs-Py-NH2 (0.10%)

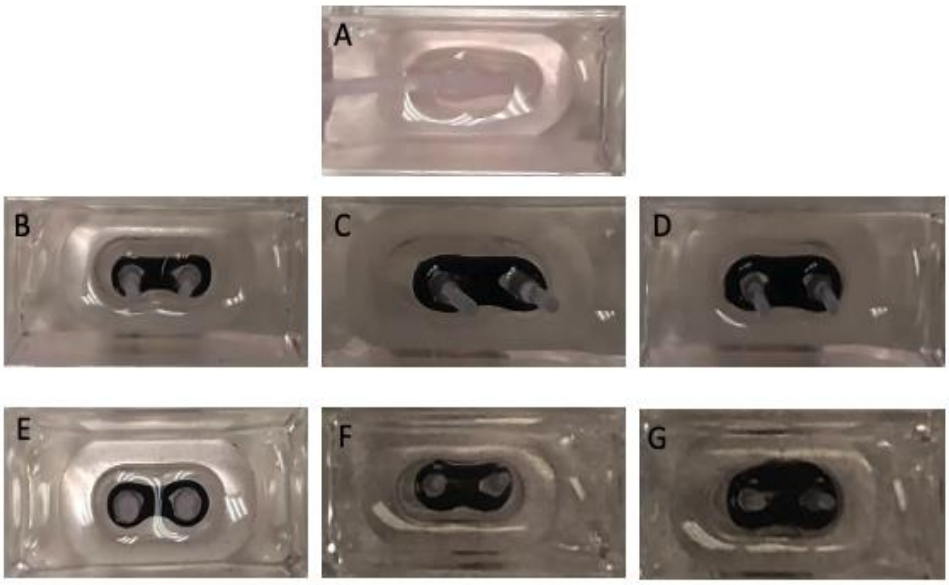

3.2.2 Electrical conductivity test of ECTs

Our group previously reported that the development of ECT using chitosan-functionalized CNTs improves wound healing and re-epithelization(75). Another study by our group showed that adding CNTs to ECTs with collagen matrix could improve several of their biomechanical characteristics, including tissue stiffness, elasticity, toughness, and extensibility(81). However, the electrical conductivity of ECT is very

important for effective application in tissue engineering, electrical transfer through the tissue improves tissue repair and stimulates growth and cellular activity by enhancing cell differentiations (91-93).

The extracellular matrix in natural tissues serves as a 3D environment for tissue development, and human tissues are more complex in structures than monolayers of cells. It is now appreciated that the 3D environment demonstrates unique effects on cell behavior as compared to 2D environments, including cell migration, proliferation, and differentiation. 3D biomaterials were required to simulate the native extracellular matrix. Hydrogels and porous scaffolds are now the most studied 3D biomaterials forms (83). In this study, prepared 3D chemically cross-linked macro-sized porous f-MWCNTs with chitosan scaffolds. the formation of a three-dimensional network of f-MWCNTs within the collagen matrix was linked to a significant increase in tissue electrical conductivity that was kind and concentration-dependent, as in MWCNT-COOH and MWCNT-NH2 the conductivity was increased when increasing the concentration of f-MWCNTs, (scheme 8).

Scheme 8

Average electrical conductivity of ECT structures of primary dermal fibroblast cells with different A)MWCNT-COOH loading and B)MWCNT-NH2 loading. The symbol (*) indicates significance ($P \leq 0.05$) compared to the control (0.000%). The two-way ANOVA was used to determine the statistical significance

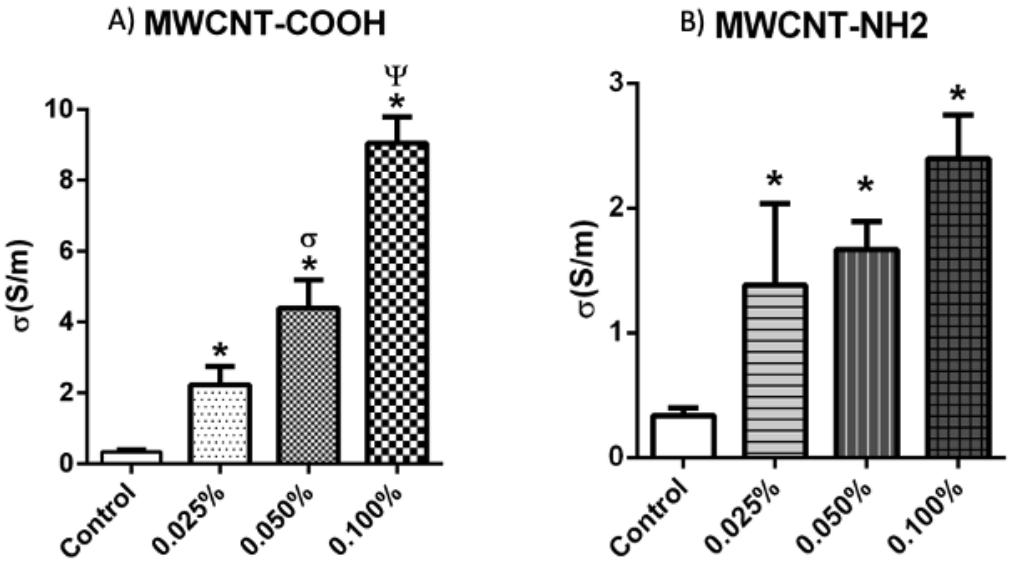

As expected, data showed that enriching tissues with f-MWCNTs significantly raised the electrical conductivity of the ECTs as compared to the control (collagen-only ECTs) which is consistent with a previous report by our lab (98). Conductivity enhancement was greater with MWCNTs- COOH compared to MWCNTs-NH2, as the conductivity of ECT with 0.1% MWCNT-COOH loading is approximately 9 s/m, but the conductivity with 0.1% MWCNT-NH2 loading is between 2-3s/m, therefore we opt to proceed with the MWCNT-COOH for the next experiments and to use the lowest tested concentration (0.025%).

The concentration of 0.025% of MWCNT-COOH was enough to sufficiently enhance the electrical conductivity of the tissue compared to the control tissue as reported in previous literature, however, this concentration was still associated with some cytotoxicity (98), which could arise from the uptake of CNTs by the cells and the associated oxidative stress reactions (99), therefore we decided to incorporate a biocompatible polymer that can coat the CNTs, enhance their distribution and sticking in the ECM, and for that we selected chitosan and tested its effect first of the tissue conductivity.

Scheme 9

Average electrical conductivity of ECT structures of primary dermal fibroblast cells with different Chitosan and 0.025% MWCNT-COOH loading. The symbol (*) indicates significance ($P \leq 0.05$) compared to the control (0.000%). The two-way ANOVA was used to determine the statistical significance

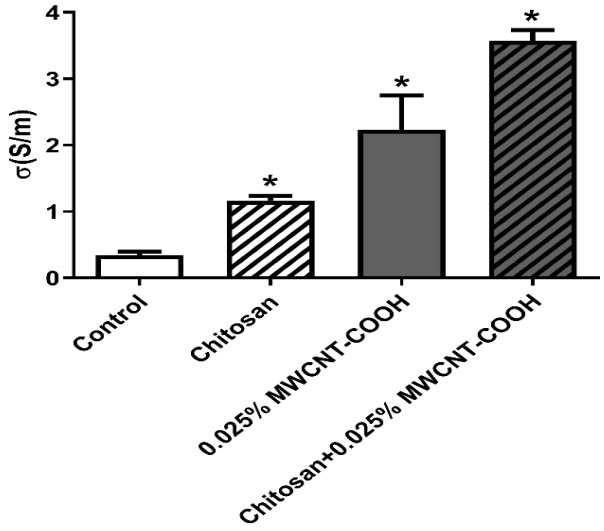

Interestingly, the data demonstrated that chitosan not only did not decrease but instead enhanced the conductivity of 0.025% MWCNTs-COOH (Scheme 9). Therefore, we tested its effect on cell viability in the next step.

3.2.3 Cell viability test (MTS assay)

Primary dermal fibroblast cells were incubated in monolayer and cultures for 24 hours in culture media containing several treatment conditions at doses equivalent to those used in ECT. The viability of primary dermal fibroblast cells was investigated through subjective visual microscopic evaluation concerning cell morphology and by MTS assay. The control cells and those treated with 0.025% of MWCNT-COOH or 0.025% MWCNTs with Chitosan loading appeared normal, spread, and well-adhered to the plastic surface, as shown in (figure 3.4). However, higher MWCNT-COOH concentrations, caused some of the cells' morphologies to be abnormal and the cells to appear less spread out over the plastic surface. Such variations appeared to depend on concentration.

Figure 3.4

Bright-field images at 100× for primary dermal fibroblast cells treated with A) Control (cells without treatment); B cells treated with Chitosan, C) 0.025%MWCNT-COOH with Chitosan, D-F) different concentrations of MWCNT-COOH (0.025%, 0.050%, and 0.100%) respectively

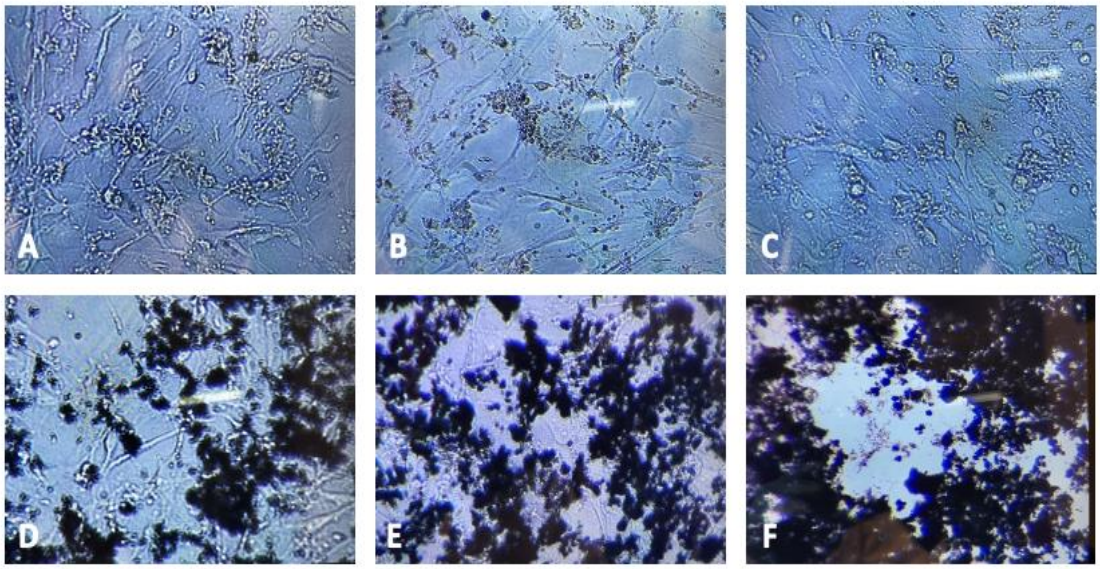

Scheme 10

Concentration-dependent effect of MWCNTs and Chitosan on the viability of primary dermal fibroblast cells over 24 hours. The symbol (*) indicates significance ($P \leq 0.05$) compared to the control (0.000%). The two-way ANOVA was used to determine the statistical significance

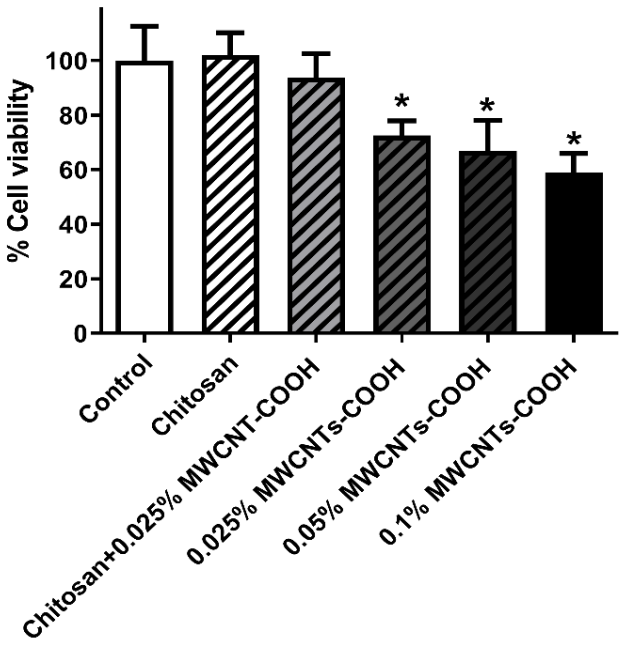

The results of the MTS analysis (Scheme 10) showed that there was a statistically significant concentration-dependent reduction in the viability of primary dermal fibroblast cells with MWCNT-COOH compared to the control cells, the concentrations of 0.025% of MWCNTs reduced the cell viability by around (20-30)%. While there was no significant reduction in viability when adding Chitosan to 0.025%MWCNT-COOH, which indicates that chitosan might have a cytoprotective effect against CNT-induced toxicity. Therefore, it can be concluded that the addition of chitosan to the matrix of the ECTs can provide two advantages; a cytoprotective effect and enhancement of electrical conductivity.

Chapter Four

Discussions and Conclusions

4.1 Conclusion

MWCNTs have been successfully functionalized noncovalently, and a good dispersibility of functionalization was demonstrated. The pristine MWCNTs form aggregates and precipitate immediately whereas the functionalized MWCNTs with py-COOH or Py-NH_2 showed good water dispersibility and stability. The successful π-π stacking between the carbon nanotubes and the pyrene moieties was confirmed by atomic force microscope (AFM). The successful functionalization of the carbon nanotubes with the successful separation of the nanotubes.

Primary dermal fibroblast cells extracted from mice skin and ECTs including these primary cells were created, collagen hydrogel that is fortified by MWCNTs which are noncovalently functionalization with pyrene moiety and coated with chitosan was tested as a scaffold for connective engineering. Our data demonstrated that the enrichment of the ECTs with the f-MWCNTs significantly increased the electrical conductivity of the tissues in a kind and concentration-dependent manner, and conductivity enhancement was greater with MWCNTs- COOH compared to MWCNTs-NH2.

The results of the MTS analysis showed that there was a statistically significant concentration-dependent reduction in the viability of primary dermal fibroblast cells with MWCNT-COOH compared to the control cells, higher MWCNT-COOH concentrations, caused some of the cells' morphologies to be abnormal and the cells to appear less spread out over the plastic surface. The concentration of 0.025% of MWCNT-COOH was enough to sufficiently enhance the electrical conductivity of the tissue. However, this concentration was still associated with some cytotoxicity relative to the control, while there was no significant reduction in viability when adding chitosan to 0.025%MWCNT-COOH but also enhanced the electrical conductivity, which indicates that chitosan might have a cytoprotective effect in addition to electrical conductivity enhancement.

The results expected that such a scaffold could be applicable broadly in future biomaterial designs as a scaffold for connective and cardiac tissue engineering, and demonstrated great potential for additional in vivo studies.

List of abbreviations

Abbreviation	Meaning
CDCl3	Deuterochloroform
CHCl3	Chloroform
CNTs	Carbon nanotubes
COOH	Carboxylic acid
DCM	Dichloromethane
DMAP	4-Dimethylaminopyridine
DMEM	Dulbecco's Modified Eagle's Medium
ECM	Extracellular matrix
ECTs	Engineered connective tissues
EDC	1-Ethyl-3-(3-dimethylaminopropyl)carbodiimide hydrochloride
Et3N	Trimethylamine
FBS	Fetal bovine serum
f-MWCNTs	Functionalized multi-walled carbon nanotubes
H2	Hydrogen gas
H2O	Water
HCl	Hydrochloride
MeOH	Methanol
MTS	3-(4,5-dimethylthiazol-2-yl)-5-(3-carboxymethoxyphenyl)-2-(4-sulfophenyl)-2H-tetrazolium
MWCNT	Multi-walled carbon nanotube
NaHCO3	Sodium bicarbonate
NaOH	Sodium hydroxide
Na2SO4	Sodium sulfate
NMR	Nuclear Magnetic Resonance
^{O}C	Degree Celsius
OH	Hydroxyl
PBS	Phosphate buffer saline
Pen-Strep	Penicillin-streptomycin
pH	Power of hydrogen
PLGA	*poly(lactic-co-glycolic acid)*
SEM	Scanning electron microscope
SWCNT	Single-walled carbon nanotubes
TEG	Tetraethylene glycol
THF	Tetrahydrofuran
TLC	Thin layer chromatography
w/v	Weight by volume
v/v	Volume by volume

References

[1] Williams JK, Andersson K-E. Regenerative pharmacology: recent developments and future perspectives. Regenerative medicine. 2016;11(8):859-70.

[2] Engel E, Michiardi A, Navarro M, Lacroix D, Planell JA. Nanotechnology in regenerative medicine: the materials side. Trends in biotechnology. 2008;26(1):39-47.

[3] Petit-Zeman S. Regenerative medicine. Nature biotechnology. 2001;19(3):201-6.

[4] PIECHOTA HJ, DAHMS SE, NUNES LS, DAHIYA R, LUE TF, TANAGHO EA. In vitro functional properties of the rat bladder regenerated by the bladder acellular matrix graft. The Journal of urology. 1998;159(5):1717-24.

[5] Yoo JJ, Meng J, Oberpenning F, Atala A. Bladder augmentation using allogenic bladder submucosa seeded with cells. Urology. 1998;51(2):221-5.

[6] Adamowicz J, Kowalczyk T, Drewa T. Tissue engineering of urinary bladder–current state of art and future perspectives. Central European journal of urology. 2013;66(2):202.

[7] Sikavitsas VI, Bancroft GN, Mikos AG. Formation of three-dimensional cell/polymer constructs for bone tissue engineering in a spinner flask and a rotating wall vessel bioreactor. Journal of Biomedical Materials Research: An Official Journal of The Society for Biomaterials, The Japanese Society for Biomaterials, and The Australian Society for Biomaterials and the Korean Society for Biomaterials. 2002;62(1):136-48.

[8] Guan S, Zhang X-L, Lin X-M, Liu T-Q, Ma X-H, Cui Z-F. Chitosan/gelatin porous scaffolds containing hyaluronic acid and heparan sulfate for neural tissue engineering. Journal of Biomaterials Science, Polymer Edition. 2013;24(8):999-1014.

[9] Murphy AR, Laslett A, O'Brien CM, Cameron NR. Scaffolds for 3D in vitro culture of neural lineage cells. Acta Biomaterialia. 2017;54:1-20.

[10] Woodard H, White D. The composition of body tissues. The British journal of radiology. 1986;59(708):1209-18.

[11] Culav EM, Clark CH, Merrilees MJ. Connective tissues: matrix composition and its relevance to physical therapy. Physical therapy. 1999;79(3):308-19.

[12] Sahoo S, Lok Toh S, Hong Goh JC. PLGA nanofiber-coated silk microfibrous scaffold for connective tissue engineering. Journal of Biomedical Materials Research Part B: Applied Biomaterials. 2010;95(1):19-28.

[13] Hasan A, Paul A, Vrana NE, Zhao X, Memic A, Hwang Y-S, et al. Microfluidic techniques for development of 3D vascularized tissue. Biomaterials. 2014;35(26):7308-25.

[14] Hasan A, Ragaert K, Swieszkowski W, Selimović Š, Paul A, Camci-Unal G, et al. Biomechanical properties of native and tissue engineered heart valve constructs. Journal of biomechanics. 2014;47(9):1949-63.

[15] Bai RG, Muthoosamy K, Manickam S, Hilal-Alnaqbi A. Graphene-based 3D scaffolds in tissue engineering: fabrication, applications, and future scope in liver tissue engineering. International journal of nanomedicine. 2019;14:5753.

[16] Wong EW, Sheehan PE, Lieber CM. Nanobeam mechanics: elasticity, strength, and toughness of nanorods and nanotubes. science. 1997;277(5334):1971-5.

[17] Esteves IA, Cruz FJ, Müller EA, Agnihotri S, Mota JP. Determination of the surface area and porosity of carbon nanotube bundles from a Langmuirian analysis of sub-and supercritical adsorption data. Carbon. 2009;47(4):948-56.

[18] Shin SR, Shin C, Memic A, Shadmehr S, Miscuglio M, Jung HY, et al. Aligned carbon nanotube–based flexible gel substrates for engineering biohybrid tissue actuators. Advanced functional materials. 2015;25(28):4486-95.

[19] MacDonald RA, Voge CM, Kariolis M, Stegemann JP. Carbon nanotubes increase the electrical conductivity of fibroblast-seeded collagen hydrogels. Acta biomaterialia. 2008;4(6):1583-92.

[20] Da Silva EE, Della Colleta HH, Ferlauto AS, Moreira RL, Resende RR, Oliveira S, et al. Nanostructured 3-D collagen/nanotube biocomposites for future bone regeneration scaffolds. Nano Research. 2009;2(6):462-73.

[21] Bianco A, Prato M. Can carbon nanotubes be considered useful tools for biological applications? Advanced Materials. 2003;15(20):1765-8.

[22] Venkatesan J, Kim S-K. Chitosan composites for bone tissue engineering—an overview. Marine drugs. 2010;8(8):2252-66.

[23] Tonelli FM, Santos AK, Gomes KN, Lorencon E, Guatimosim S, Ladeira LO, et al. Carbon nanotube interaction with extracellular matrix proteins producing scaffolds for tissue engineering. International journal of nanomedicine. 2012;7:4511.

[24] Gaur M, Misra C, Yadav AB, Swaroop S, Maolmhuaidh FÓ, Bechelany M, et al. Biomedical applications of carbon nanomaterials: fullerenes, quantum dots, nanotubes, nanofibers, and graphene. Materials. 2021;14(20):5978.

[25] Nardecchia S, Carriazo D, Ferrer ML, Gutiérrez MC, del Monte F. Three dimensional macroporous architectures and aerogels built of carbon nanotubes and/or graphene: synthesis and applications. Chemical Society Reviews. 2013;42(2):794-830.

[26] Bakry R, Vallant RM, Najam-ul-Haq M, Rainer M, Szabo Z, Huck CW, et al. Medicinal applications of fullerenes. International journal of nanomedicine. 2007;2(4):639-49.

[27] Saldmann F, Saldmann A, Lemaire MC. Characterization and internalization of nanodiamond–trehalose conjugates into mammalian fibroblast cells of naked mole rat. International Nano Letters. 2020;10:151-7.

[28] Zhang M, Zhao L, Du F, Wu Y, Cai R, Xu L, et al. Facile synthesis of cerium-doped carbon quantum dots as a highly efficient antioxidant for free radical scavenging. Nanotechnology. 2019;30(32):325101.

[29] Pyun J. Graphene oxide as catalyst: application of carbon materials beyond nanotechnology. Angewandte Chemie International Edition. 2011;50(1):46-8.

[30] Hirsch A. The era of carbon allotropes. Nature materials. 2010;9(11):868-71.

[31] Manawi YM, Samara A, Al-Ansari T, Atieh MA. A review of carbon nanomaterials' synthesis via the chemical vapor deposition (CVD) method. Materials. 2018;11(5):822.

[32] Siegal M, Overmyer D, Provencio P. Precise control of multiwall carbon nanotube diameters using thermal chemical vapor deposition. Applied physics letters. 2002;80(12):2171-3.

[33] Iijima S. Carbon nanotubes: past, present, and future. Physica B: Condensed Matter. 2002;323(1-4):1-5.

[34] Khalid M, Ratnam CT, Walvekar R, Ketabchi MR, Hoque ME. Reinforced natural rubber nanocomposites: next generation advanced material. Green Biocomposites: Springer; 2017. p. 309-45.

[35] Cheng L-C, Jiang X, Wang J, Chen C, Liu R-S. Nano–bio effects: interaction of nanomaterials with cells. Nanoscale. 2013;5(9):3547-69.

[36] Kroto HW, Heath JR, O'Brien SC, Curl RF, Smalley RE. C60: Buckminsterfullerene. nature. 1985;318(6042):162-3.

[37] Awasthi K, Srivastava A, Srivastava O. Synthesis of carbon nanotubes. Journal of nanoscience and nanotechnology. 2005;5(10):1616-36.

[38] Zhou D, Seraphin S, Wang S. Single-walled carbon nanotubes growing radially from YC2 particles. Applied physics letters. 1994;65(12):1593-5.

[39] Yuan L, Saito K, Pan C, Williams F, Gordon A. Nanotubes from methane flames. Chemical physics letters. 2001;340(3-4):237-41.

[40] Hsu W, Hare J, Terrones M, Kroto H, Walton D, Harris P. Condensed-phase nanotubes. Nature. 1995;377(6551):687-.

[41] Chen GZ, Kinloch I, Shaffer MS, Fray DJ, Windle AH. Electrochemical investigation of the formation of carbon nanotubes in molten salts. High Temperature Material Processes. 1998;2:459-70.

[42] Chen Y. Solid-state formation of carbon nanotubes. Carbon Nanotechnology. 2006:53-80.

[43] Wu H-C, Chang X, Liu L, Zhao F, Zhao Y. Chemistry of carbon nanotubes in biomedical applications. Journal of Materials Chemistry. 2010;20(6):1036-52.

[44] Jagtoyen M, Pardue J, RANTELL T, DERBYSHIRE F. Porosity of carbon nanotubes. Adsorption Science And Technology: World Scientific; 2000. p. 289-93.

[45] Meo M, Rossi M. Prediction of Young's modulus of single wall carbon nanotubes by molecular-mechanics based finite element modelling. Composites Science and Technology. 2006;66(11-12):1597-605.

[46] Peng B, Locascio M, Zapol P, Li S, Mielke SL, Schatz GC, et al. Measurements of near-ultimate strength for multiwalled carbon nanotubes and irradiation-induced crosslinking improvements. Nature nanotechnology. 2008;3(10):626-31.

[47] Zhao Q, Gan Z, Zhuang Q. Electrochemical sensors based on carbon nanotubes. Electroanalysis: An International Journal Devoted to Fundamental and Practical Aspects of Electroanalysis. 2002;14(23):1609-13.

[48] Tasis D, Tagmatarchis N, Bianco A, Prato M. Chemistry of carbon nanotubes. Chemical reviews. 2006;106(3):1105-36.

[49] Abdul-Adheem WR, Ghaffoori AJ. A Review on Carbon Nanotubes Structural Types and Techniques.

[50] Zhou Y, Fang Y, Ramasamy RP. Non-covalent functionalization of carbon nanotubes for electrochemical biosensor development. Sensors. 2019;19(2):392.

[51] Mundra RV, Wu X, Sauer J, Dordick JS, Kane RS. Nanotubes in biological applications. Current opinion in biotechnology. 2014;28:25-32.

[52] Anzar N, Hasan R, Tyagi M, Yadav N, Narang J. Carbon nanotube-A review on Synthesis, Properties and plethora of applications in the field of biomedical science. Sensors International. 2020;1:100003.

[53] Harrison BS, Atala A. Carbon nanotube applications for tissue engineering. Biomaterials. 2007;28(2):344-53.

[54] Simon J, Flahaut E, Golzio M. Overview of carbon nanotubes for biomedical applications. Materials. 2019;12(4):624.

[55] Wayu MB, Pannell MJ, Labban N, Case WS, Pollock JA, Leopold MC. Functionalized carbon nanotube adsorption interfaces for electron transfer studies of galactose oxidase. Bioelectrochemistry. 2019;125:116-26.

[56] Peng R, Tang XS, Li D. Detection of Individual Molecules and Ions by Carbon Nanotube-Based Differential Resistive Pulse Sensor. Small. 2018;14(15):1800013.

[57] Welsher K, Liu Z, Sherlock SP, Robinson JT, Chen Z, Daranciang D, et al. A route to brightly fluorescent carbon nanotubes for near-infrared imaging in mice. Nature nanotechnology. 2009;4(11):773-80.

[58] Ibrahim KS. Carbon nanotubes-properties and applications: a review. Carbon letters. 2013;14(3):131-44.

[59] Siochi EJ, Working DC, Park C, Lillehei PT, Rouse JH, Topping CC, et al. Melt processing of SWCNT-polyimide nanocomposite fibers. Composites Part B: Engineering. 2004;35(5):439-46.

[60] Rao CNR, Satishkumar B, Govindaraj A, Nath M. Nanotubes. ChemPhysChem. 2001;2(2):78-105.

[61] Reich S, Thomsen C, Maultzsch J. Carbon nanotubes: basic concepts and physical properties: John Wiley & Sons; 2004.

[62] Ema M, Gamo M, Honda K. A review of toxicity studies of single-walled carbon nanotubes in laboratory animals. Regulatory Toxicology and Pharmacology. 2016;74:42-63.

[63] Liu Z, Robinson JT, Tabakman SM, Yang K, Dai H. Carbon materials for drug delivery & cancer therapy. Materials today. 2011;14(7-8):316-23.

[64] Liu Z, Tabakman SM, Chen Z, Dai H. Preparation of carbon nanotube bioconjugates for biomedical applications. Nature protocols. 2009;4(9):1372-81.

[65] Lei J, Ju H. Nanotubes in biosensing. Wiley Interdisciplinary Reviews: Nanomedicine and Nanobiotechnology. 2010;2(5):496-509.

[66] Assali M, Leal MP, Fernández I, Romero-Gomez P, Baati R, Khiar N. Improved non-covalent biofunctionalization of multi-walled carbon nanotubes using carbohydrate amphiphiles with a butterfly-like polyaromatic tail. Nano research. 2010;3(11):764-78.

[67] Holzinger M, Vostrowsky O, Hirsch A, Hennrich F, Kappes M, Weiss R, et al. Sidewall functionalization of carbon nanotubes. Angewandte chemie international edition. 2001;40(21):4002-5.

[68] Chen RJ, Zhang Y, Wang D, Dai H. Noncovalent Sidewall Functionalization of Single-Walled Carbon Nanotubes for Protein Immobilization. Journal of the American Chemical Society. 2001;123(16):3838-9.

[69] Kuila T, Bose S, Mishra AK, Khanra P, Kim NH, Lee JH. Chemical functionalization of graphene and its applications. Progress in Materials Science. 2012;57(7):1061-105.

[70] Omurtag PS, Alkan B, Durmaz H, Hizal G, Tunca U. Indirect functionalization of multiwalled carbon nano tubes through non-covalent interaction of functional polyesters. Polymer. 2018;141:213-20.

[71] Ueno H, Yamada H, Tanaka I, Kaba N, Matsuura M, Okumura M, et al. Accelerating effects of chitosan for healing at early phase of experimental open wound in dogs. Biomaterials. 1999;20(15):1407-14.

[72] Islam S, Bhuiyan M, Islam M. Chitin and chitosan: structure, properties and applications in biomedical engineering. Journal of Polymers and the Environment. 2017;25(3):854-66.

[73] Bartone FF, Adickes ED. Chitosan: effects on wound healing in urogenital tissue: preliminary report. The Journal of Urology. 1988;140(5):1134-7.

[74] Biagini G, Bertani A, Muzzarelli R, Damadei A, DiBenedetto G, Belligolli A, et al. Wound management with N-carboxybutyl chitosan. Biomaterials. 1991;12(3):281-6.

[75] Kittana N, Assali M, Abu-Rass H, Lutz S, Hindawi R, Ghannam L, et al. Enhancement of wound healing by single-wall/multi-wall carbon nanotubes complexed with chitosan. International Journal of Nanomedicine. 2018;13:7195.

[76] Hirata E, Uo M, Takita H, Akasaka T, Watari F, Yokoyama A. Multiwalled carbon nanotube-coating of 3D collagen scaffolds for bone tissue engineering. Carbon. 2011;49(10):3284-91.

[77] Mikael PE, Amini AR, Basu J, Arellano-Jimenez MJ, Laurencin CT, Sanders MM, et al. Functionalized carbon nanotube reinforced scaffolds for bone regenerative engineering: fabrication, in vitro and in vivo evaluation. Biomedical Materials. 2014;9(3):035001.

[78] Lalwani G, Gopalan A, D'Agati M, Srinivas Sankaran J, Judex S, Qin YX, et al. Porous three-dimensional carbon nanotube scaffolds for tissue engineering. Journal of Biomedical Materials Research Part A. 2015;103(10):3212-25.

[79] Gholizadeh S, Moztarzadeh F, Haghighipour N, Ghazizadeh L, Baghbani F, Shokrgozar MA, et al. Preparation and characterization of novel functionalized multiwalled carbon nanotubes/chitosan/β-Glycerophosphate scaffolds for bone tissue engineering. International journal of biological macromolecules. 2017;97:365-72.

[80] Martinelli V, Bosi S, Peña B, Baj G, Long CS, Sbaizero O, et al. 3D carbon-nanotube-based composites for cardiac tissue engineering. ACS Applied Bio Materials. 2018;1(5):1530-7.

[81] Kittana N, Assali M, Zimmermann W-H, Liaw N, Santos GL, Rehman A, et al. Modulating the Biomechanical Properties of Engineered Connective Tissues by Chitosan-Coated Multiwall Carbon Nanotubes. International journal of nanomedicine. 2021;16:989.

[82] Tondnevis F, Keshvari H, Mohandesi JA. Fabrication, characterization, and in vitro evaluation of electrospun polyurethane-gelatin-carbon nanotube scaffolds for cardiovascular tissue engineering applications. Journal of Biomedical Materials Research Part B: Applied Biomaterials. 2020;108(5):2276-93.

[83] Dong R, Ma PX, Guo B. Conductive biomaterials for muscle tissue engineering. Biomaterials. 2020;229:119584.

[84] Dong R, Zhao X, Guo B, Ma PX. Self-healing conductive injectable hydrogels with antibacterial activity as cell delivery carrier for cardiac cell therapy. ACS applied materials & interfaces. 2016;8(27):17138-50.

[85] Xie M, Wang L, Guo B, Wang Z, Chen YE, Ma PX. Ductile electroactive biodegradable hyperbranched polylactide copolymers enhancing myoblast differentiation. Biomaterials. 2015;71:158-67.

[86] Wu Y, Wang L, Guo B, Shao Y, Ma PX. Electroactive biodegradable polyurethane significantly enhanced Schwann cells myelin gene expression and neurotrophin secretion for peripheral nerve tissue engineering. Biomaterials. 2016;87:18-31.

[87] Baniasadi H, SA AR, Mashayekhan S. Fabrication and characterization of conductive chitosan/gelatin-based scaffolds for nerve tissue engineering. International journal of biological macromolecules. 2015;74:360-6.

[88] Kabiri M, Oraee-Yazdani S, Dodel M, Hanaee-Ahvaz H, Soudi S, Seyedjafari E, et al. Cytocompatibility of a conductive nanofibrous carbon nanotube/poly (L-Lactic acid) composite scaffold intended for nerve tissue engineering. EXCLI journal. 2015;14:851.

[89] Yazdimamaghani M, Razavi M, Mozafari M, Vashaee D, Kotturi H, Tayebi L. Biomineralization and biocompatibility studies of bone conductive scaffolds containing poly (3, 4-ethylenedioxythiophene): poly (4-styrene sulfonate)(PEDOT: PSS). Journal of materials science: Materials in Medicine. 2015;26(12):1-11.

[90] Hardy JG, Geissler SA, Aguilar Jr D, Villancio-Wolter MK, Mouser DJ, Sukhavasi RC, et al. Instructive Conductive 3D Silk Foam-Based Bone Tissue Scaffolds Enable Electrical Stimulation of Stem Cells for Enhanced Osteogenic Differentiation. Macromolecular Bioscience. 2015;15(11):1490-6.

[91] Ntege EH, Sunami H, Shimizu Y. Advances in regenerative therapy: a review of the literature and future directions. Regenerative therapy. 2020;14:136-53.

[92] Jin G, Li K. The electrically conductive scaffold as the skeleton of stem cell niche in regenerative medicine. Materials Science and Engineering: C. 2014;45:671-81.

[93] Breukers R, Gilmore K, Kita M, Wagner K, Higgins M, Moulton S, et al. Creating conductive structures for cell growth: Growth and alignment of myogenic cell types on polythiophenes. Journal of Biomedical Materials Research Part A. 2010;95(1):256-68.

[94] Assali M, Kittana N, Alhaj-Qasem S, Hajjyahya M, Abu-Rass H, Alshaer W, et al. Noncovalent functionalization of carbon nanotubes as a scaffold for tissue engineering. Scientific Reports. 2022;12(1):1-17.

[95] Alsouqi DG. Functionalization of graphene sheets and their antibacterial activity: An-Najah National University; 2017.

[96] دفم رشدي ,حمد. Bio-Functionalization of SWCNTs with Combretastatin A4 for Targeted Cancer Therapy: An-Najah National University; 2017.

[97] Qasem S. Noncovalent Functionalization of Carbon Nanomaterials as a Scaffold for Tissue Engineering: 2020 ;جامعة النجاح الوطنية.

[98] Assali M, Kittana N, Alhaj-Qasem S, Hajjyahya M, Abu-Rass H, Alshaer W, et al. Noncovalent functionalization of carbon nanotubes as a scaffold for tissue engineering. Sci Rep. 2022;12(1):12062.

[99] Rasras S, Kalantari H, Rezaei M, Dehghani MA, Zeidooni L, Alikarami K, et al. Single-walled and multiwalled carbon nanotubes induce oxidative stress in isolated rat brain mitochondria. Toxicol Ind Health. 2019;35(7):497-506.

Appendices

Appendix A

Figures of Study

Figure A.1

Noncovalent functionalization of MWCNTs with Py-COOH and Py-NH2

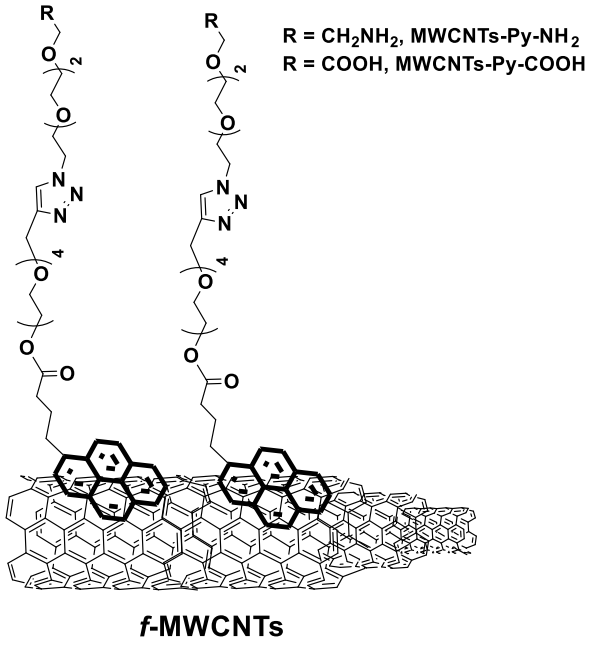

Figure A.2

48-well plate with stretchers

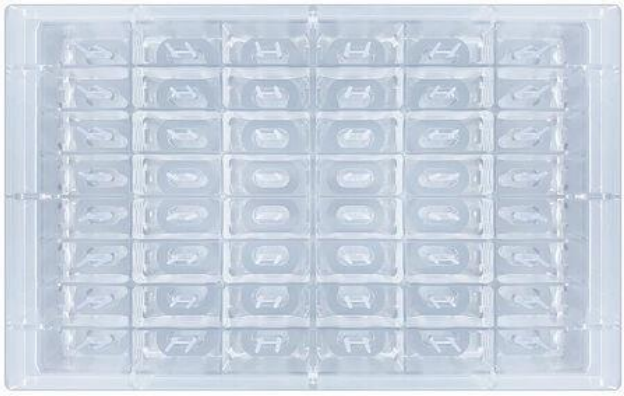

جـامعـــة النجاح الوطنية
كليـــة الدراســـات العليـــا

تطوير هيكل بنائي محسن لهندسة الانسجة مرتكز على التفعيل غير التناسقي لمواد النانو الكربونية

إعداد
سلسبيل مأمون جميل عوده

إشراف
د. محي الدين العسالي
د. نعيم كتانة

قدمت هذه الرسالة استكمالا لمتطلبات الحصول على درجة الماجستير في العلوم الصيدلانية، من كلية الدراسات العليا، في جامعة النجاح الوطنية، نابلس– فلسطين.

2022

تطوير هيكل بنائي محسن لهندسة الانسجة مرتكز على التفعيل غير التناسقي لمواد النانو الكربونية

إعداد

سلسبيل مأمون جميل عوده

إشراف

د. محي الدين العسالي

د. نعيم كتانة

الملخص

تتضمن إحدى الطرق الرئيسية لهندسة الأنسجة للأغراض العلاجية استخدام الخلايا الأولية التي يتم تربيتها على سقالة متوافقة حيوياً ذات الخصائص المناسبة. تهدف هذه الأنسجة إلى الحفاظ على و/ أو استعادة وظائف الأنسجة الطبيعية. على مدى السنوات القليلة الماضية، تم إيلاء اهتمام كبير للمواد النانوية الكربونية، مثل الأنابيب النانوية الكربونية (CNTs)، وتطبيقاتها المحتملة في توليد سقالات الأنسجة لضبتها بعض الخصائص الفيزيائية للأنسجة مثل المرونة والليونة والمسامية.

كانت العقبة الرئيسية أمام استخدام الأنابيب النانوية الكربونية في التطبيقات البيولوجية هي انخفاض قابلية الذوبان في الماء والسمية الخلوية، ومع ذلك، فقد وجد أن تفعيل الأنابيب النانوية الكربونية بشكل مناسب مع المجموعات الوظيفية القطبية يمكن أن يحل هذه المشكلة ويحسن توافقها الحيوي. يمكن تحقيق فوائد مماثلة عن طريق طلاء الأنابيب النانوية الكربونية بالشيتوزان، وهو قابل للتحلل البيولوجي، ومتوافق حيويًا، ويمكن أن يشكل هياكل مسامية مناسبة لنمو الخلايا.

ولذلك، في مشروعنا، نهدف إلى التحقق في خصائص النسيج الضام الهندسي (ECTs) الذي يتكون من الخلايا الليفية الجلدية الأولية وهيدروجيل الكولاجين المشبع بتراكيز مختلفة من التفعيل غير التساهمي

للمواد النانوية الكربونية متعددة الجدران (MWCNTs) مع جزء البيرين ومغلف بـ الشيتوزان. كانت التراكيز المختبرة 0.025٪، 0.05٪، 0.1٪.

أظهرت بياناتنا أن إثراء الانسجة الضامة المهندسة (ECTs) باستخدام الأنابيب النانونية الكربونية متعددة الجدران المفعلة (functionalized MWCNT) زاد بشكل كبير من الموصلية الكهربائية للأنسجة بطريقة تعتمد على النوع والتركيز. علاوة على ذلك، كان تحسين الموصلية أكبر مع MWCNTs-COOH مقارنة بـ MWCNTs-NH2، وكان تركيز 0.025 ٪ من MWCNT-COOH كافياً لتعزيز الموصلية الكهربائية للنسيج بشكل كافٍ مقارنة بالأنسجة التي تحتوي فقط على الخلايا. ومع ذلك، لا يزال هذا التركيز مرتبطًا ببعض السمية الخلوية حيث يقلل من قابلية الخلية للبقاء بحوالي (20–30) ٪ بالنسبة إلى الأنسجة الخالية من الأنابيب النانونية الكربونية، بينما لم يكن هناك انخفاض كبير في الخلايا عند إضافة الشيتوزان إلى 0.025 ٪ MWCNT-COOH، مما يشير إلى أن قد يكون للشيتوزان تأثير واقي للخلايا ضد السمية التي تسببها الأنابيب النانونية الكربونية، بالإضافة إلى تعزيز الموصلية الكهربائي.

الكلمات المفتاحية: هندسة الانسجة، مواد النانو الكربونية، شيتوزان، الخلايا الليفية الجلدية الأولية.